Origins of East Asian Summer Monsoon Seasonality®

J. C. H. CHIANG AND W. KONG

Department of Geography and Berkeley Atmospheric Sciences Center, University of California, Berkeley, California

C. H. WU

Research Center for Environmental Changes, Academia Sinica, Taipei, Taiwan

D. S. BATTISTI

Department of Atmospheric Sciences, University of Washington, Seattle, Washington

(Manuscript received 27 November 2019, in final form 27 March 2020)

ABSTRACT

The East Asian summer monsoon is unique among summer monsoon systems in its complex seasonality, exhibiting distinct intraseasonal stages. Previous studies have alluded to the downstream influence of the westerlies flowing around the Tibetan Plateau as key to its existence. We explore this hypothesis using an atmospheric general circulation model that simulates the intraseasonal stages with fidelity. Without a Tibetan Plateau, East Asia exhibits only one primary convective stage typical of other monsoons. As the plateau is introduced, the distinct rainfall stages-spring, pre-mei-yu, mei-yu, and midsummer-emerge, and rainfall becomes more intense overall. This emergence coincides with a pronounced modulation of the westerlies around the plateau and extratropical northerlies penetrating northeastern China. The northerlies meridionally constrain the moist southerly flow originating from the tropics, leading to a band of lower-tropospheric convergence and humidity front that produces the rainband. The northward migration of the westerlies away from the northern edge of the plateau leads to a weakening of the extratropical northerlies, which, coupled with stronger monsoonal southerlies, leads to the northward migration of the rainband. When the peak westerlies migrate north of the plateau during the midsummer stage, the extratropical northerlies disappear, leaving only the monsoon low-level circulation that penetrates northeastern China; the rainband disappears, leaving isolated convective rainfall over northeastern China. In short, East Asian rainfall seasonality results from the interaction of two seasonally evolving circulations—the monsoonal southerlies that strengthen and extend northward, and the midlatitude northerlies that weaken and eventually disappear—as summer progresses.

1. Introduction

The East Asian summer monsoon is unique among monsoon systems for its complex seasonality. While the other monsoons are characterized by a single major onset and retreat of convective rainfall in the early summer and fall respectively, early summer rainfall over East Asia is characterized by a southwest-to-northeast oriented rain belt extending from eastern China toward

© Supplemental information related to this paper is available at the Journals Online website: https://doi.org/10.1175/JCLI-D-19-0888.s1.

Corresponding author: John Chiang, jch_chiang@berkeley.edu

Japan; this is the well-known mei-yu rainband. The seasonal migration of this rainfall is marked by distinct quasi-stationary stages with abrupt transitions in between (Ding and Chan 2005, and references therein). A Hovmöller plot of the rainfall climatology over East Asia 110°–120°E (Fig. 1a) succinctly shows the nature and timing of the intraseasonal stages. The already significant rainfall over southern China during the spring—which is persistent in nature (Wu et al. 2007)—gives way to the pre-mei-yu stage starting in early May marked by the beginning of convective rainfall surges over the South China Sea and southeastern China. The mei-yu stage begins in early to mid-June with a rapid northward progression of the rainfall to central China. This quasi-stationary stage lasts for 20–30 days, after which

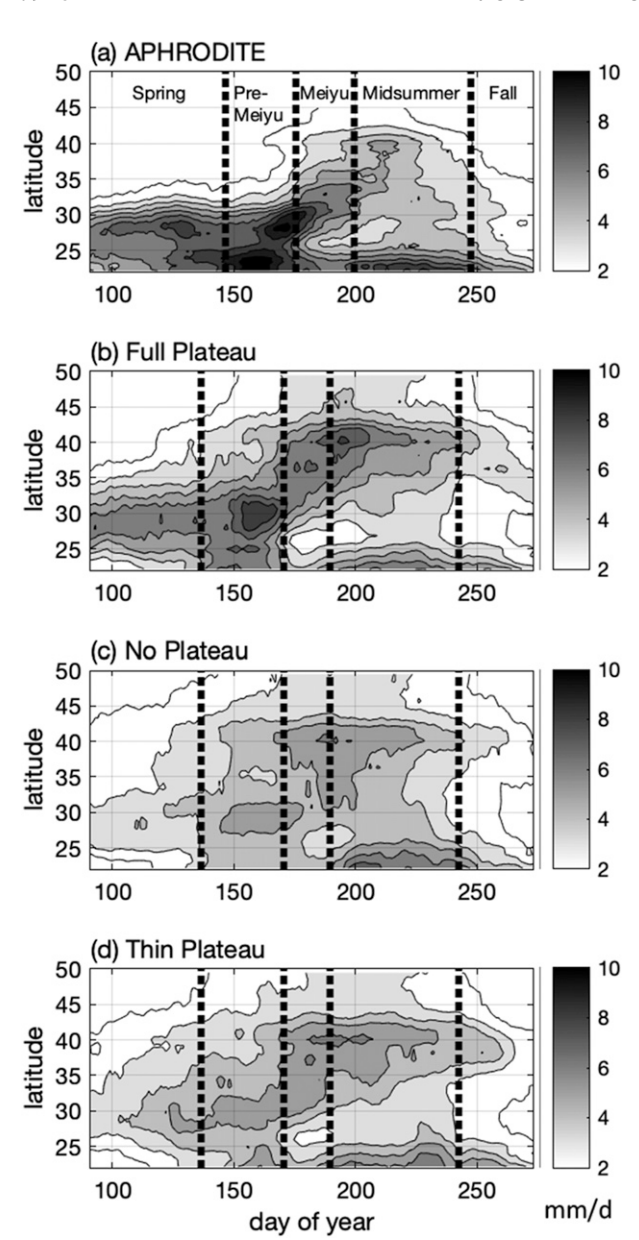


FIG. 1. (a) Latitude-time section of land rainfall (mm day⁻¹; contour interval is 1 mm day⁻¹) over eastern China (110°-120°E), and from April to September averaged for 1951-2007, using the APHRODITE rainfall dataset (Yatagai et al. 2012). A 15-day running mean is applied prior to plotting. Only contours above 2 mm day⁻¹ are drawn, and regions of heavier rainfall (>3 mm day⁻¹) are shaded. Also marked (vertical dashed lines) are the seasonal stages in the rainfall. Timing of the stages comes from a SOM analysis on APHRODITE rainfall, as reported in Chiang et al. 2017. (b) As in (a), but from the CAM5 Full Plateau simulation [note that rainfall over ocean points here are masked out to be consistent with (a)]. (c) As in (b), but for the No Plateau simulation. (d) As in (b), but for the Thin Plateau simulation. The timings for the intraseasonal stages shown in (b) and (c) are derived from a SOM analysis of Full Plateau precipitation; see text for details.

the rainfall abruptly jumps to northern China and the Korean peninsula around early-mid July. This mid-summer stage exists for about a month, before the rainfall transitions back south. Furthermore, the pre-mei-yu and mei-yu rainfall are primarily from "banded" rainfall resulting from large-scale frontal convergence, whereas midsummer rainfall results from local convection (Day et al. 2018). This complex seasonality has been extensively documented in the literature (e.g., see Ding and Chan 2005), but a compelling dynamical explanation of why these distinct stages exist is lacking.

Why is the East Asian rainfall seasonality so distinct? Traditionally, East Asia is regarded as a monsoon system, with an emphasis on land-ocean contrasts driving low-level monsoonal flows that brings moisture into the continent. Geographically, the large Asian continental landmass is more poleward than is typical for monsoonal systems, and the East Asian monsoon region in particular occupies the subtropical latitudes. As discussed in Rodwell and Hoskins (2001), these "subtropical monsoons" occur at the eastern edge of the continents and are closely associated with oceanic anticyclones to its east, as the monsoonal flow is tied to the zonal pressure contrast between this anticyclone with the monsoonal cyclone to its west. Indeed, the strength and positioning of the western North Pacific high features prominently in East Asian summer monsoon studies. As summer begins in the Northern Hemisphere, the Asian landmass heats up faster than the oceans, leading to a pressure contrast between the Asian landmass and North Pacific subtropical high. Diabatic heating associated with the existence of the Tibetan Plateau has been proposed to be a dominant thermodynamic driver of the East Asian monsoon system (Flohn 1968; Li and Yanai 1996). As the season progresses beyond summer, the land cools down relative to the ocean and the thermal contrast reverses, giving rise to the East Asian winter monsoon.

An alternative view of East Asian rainfall seasonality comes from considering the upper-level westerly circulation. East Asia is sufficiently far north that it is in the latitude of the westerlies even in the early summer. Moreover, the Tibetan Plateau upstream of East Asia serves to deflect the westerlies (either mechanically or through diabatic heating associated with the plateau), generating downstream stationary eddy circulations that interact with the monsoonal flows. The importance of the topographic effect of the westerly flow around the plateau on the East Asian monsoon has been long understood (Staff Members 1957; Yeh et al. 1959). Seasonally, the westerlies migrate from south of the plateau during the spring stage to north of the plateau by the midsummer stage, and then back to the south in the fall (Schiemann et al. 2009). This migration leads to

seasonally varying downstream circulation over East Asia, providing another source of seasonality. Indeed, early studies have noted the consistent relationship between the summer seasonal stages and specific configuration of the westerlies over East Asia [as highlighted in Yanai and Wu (2006); see also references therein]. The onset of the mei-yu coincides with the timing of the disappearance of the westerlies to the south of the Tibetan Plateau, and the end of the mei-yu coincides with the disappearance of the westerly jet near 35°N over Japan (Staff Members 1957), presumably due to a northward shift in the westerlies; the transition from midsummer to fall coincides with the reappearance of the jet over Japan. Recent studies have provided dynamical evidence for the importance of the westerlies in determining the existence of specific stages, including the spring (Park et al. 2012; Wu et al. 2007) and mei-yu (Chen and Bordoni 2014; Sampe and Xie 2010). Chiang et al. (2015) proposed that paleoclimate changes to the East Asian summer monsoon are tied to changes in the timing and duration of the seasonal transitions, driven by changes to the meridional position of the westerlies relative to the Tibetan Plateau.

These observations lead to a simple and intuitive idea that differences between the East Asian summer monsoon seasonality from the other monsoons originate because of the downstream effects of the westerlies impinging on the Tibetan Plateau, that then interacts with the subtropical monsoon flow. In this view, the origins of the seasonal stages depend on the specific configuration of the westerlies relative to the plateau. Molnar et al. (2010) first proposed this hypothesis, as follows:

With the seasonal decrease in the equator-to-pole temperature gradient, the jet moves northward from its winter position south of Tibet to pass directly over the plateau and then north of it. . . . In turn, the locus of convergence of moisture and precipitation downstream of the plateau, the Meiyu Front, shifts northward into central China. In this view, the intensification and northward movement of the Meiyu Front from late winter to late spring can be seen as a result of 1) the jet interacting with the plateau and 2) the increasing humidity of air that is swept in from the south over a warming ocean. . . . Then approximately when the core of the jet stream moves northward to pass north of Tibet . . . , the Meiyu Front disintegrates, and precipitation over China decreases (p. 91).

This hypothesis is appealing for several reasons. It dynamically links the observed coincidence between changes to the westerly configuration with the transition from one stage to another; also, as Molnar et al. (2010) point out, it can explain the demise of the mei-yu in late June, despite the thermal driving of the monsoon suggesting the opposite should occur. It also explains the

transition from the banded nature rainfall in the premei-yu and mei-yu, to the more local convective nature during the midsummer (Day et al. 2018). However, this hypothesis lacks specific details on what exactly it is about the westerlies that determine the nature of each seasonal stage, and why.

The proposed role of westerlies stands in contrast to the prevailing notion that emphasizes thermal forcing of the East Asian summer monsoon, in particular elevated sensible heating over the Tibetan Plateau (Staff Members 1958; Flohn 1957, 1960). A number of studies now attribute the onset of convection over the Bay of Bengal and South China Sea (marking the onset of the pre-mei-yu stage) to plateau thermal heating that causes a reversal in the meridional temperature gradient to the south of the plateau, and the consequent reversal of the upper tropospheric winds over the South China Sea and Indochina Peninsula (He et al. 1987). Ding and Chan (2005) propose one conceptual model in which the seasonal evolution of thermal forcing provides the impetus for evolving from one seasonal stage to the next, but other influences trigger the actual transition. However, the physics that could link thermal forcing to the existence and timing of the later seasonal stages is neither well developed nor understood. Notably, a recent idealized modeling study contrasting the relative roles of dynamic forcing by Tibetan Plateau topography, elevated heating, and land-ocean thermal contrast on the East Asian summer monsoon precipitation found that the majority (65%) of the rainfall can be attributed to the former, thus challenging the presumed dominant role of thermal forcing (Son et al. 2019).

Kong and Chiang (2019) substantiated one part of the Molnar et al. (2010) hypothesis, that the termination of the mei-yu rainband occurs when the jet stream moves north of the Tibetan Plateau. They found that the meiyu stage occurred when the latitude of the jet core straddled ~40°N, and it terminated when the core moved north of it. They furthermore associated the disappearance of the mei-yu rainband with the disappearance of tropospheric northerlies over northeastern China, through weakening the meridional contrast of equivalent potential temperature over central China, and also weakening the lower-tropospheric meridional wind convergence. The disappearance of the northerlies was argued to be dynamically linked to the reduced topographic forcing of the Tibetan Plateau on the westerlies, as the latter shifts north of the plateau.

In this study, we expand on this framework to address the origins of the complex seasonality of the East Asian summer monsoon in its entirety, using the Molnar et al. (2010) hypothesis as a starting point. We use an atmospheric general circulation model (AGCM) that

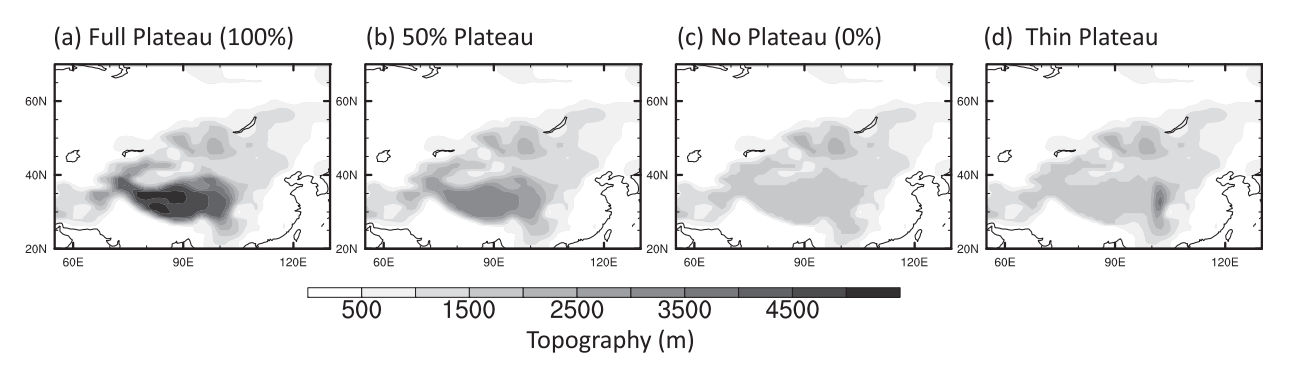


FIG. 2. Topography used in the (a) Full Plateau (100%), (b) 50%, and (c) No Plateau (0%) simulations. For 0%, the topography over the Tibetan Plateau and Himalayas are limited to 1500 m. For 50%, topography over the Tibetan Plateau and Himalayas is set to 50% of the difference between 1500 m and actual height. (d) Topography used in the Thin Plateau simulation—set to actual height east of 100°E, and to 0% to the west of 100°E.

reproduces the intraseasonal transitions to explore the role of the Tibetan Plateau. We furthermore design a set of idealized simulations to test the relative roles of the continental landmass and Tibetan Plateau in configuring the seasonality. The central idea we advance is that the complex seasonality is a result of two interacting and seasonally evolving circulations over East Asia: a moist and warm southerly monsoonal flow originating from the tropics that increases in strength as summer progresses, and an extratropical cold and dry northerly flow resulting from the influence of the Tibetan Plateau both mechanical and thermal—on the impinging westerlies, and which weakens as summer progresses. The tropical southerlies and extratropical northerlies converge to form a dynamical humidity front that determines the location of the pre-mei-yu/mei-yu rainband, and the resulting diabatic heating in turn drives a tropical southerly flow that helps maintain the rainband. The migration of the core westerlies to the north of the plateau during the midsummer stage leads to the demise of the extratropical northerlies, leaving only the monsoonal flow remaining.

The paper proceeds as follows. In section 2, we introduce the AGCM and its simulation of the East Asian monsoon; using a model that can realistically simulate the intraseasonal transitions is essential to our study. In section 3, we employ the model to show that the Tibetan Plateau is directly responsible for the intraseasonal transitions. We then explicitly demonstrate the role of the stationary eddy circulation induced by the plateau in setting the seasonality (section 4). In section 5, we offer an interpretation of the East Asian monsoon seasonality in terms of the interaction between the evolving stationary eddy circulation and monsoonal flow. In section 6, we introduce a set of idealized model simulations that illustrate the basic ingredients of East Asian monsoon seasonality. We summarize our findings in section 7.

2. Model setup and climatology

a. Model description and simulations

We use the National Center for Atmospheric Research's Community Earth System Model version 1.2.2.1 (CESM1; Hurrell et al. 2013) that has been demonstrated to simulate the intraseasonal stages of the East Asian summer monsoon with fidelity (Chiang et al. 2015). The component set used (F_1850_CAM5) includes the coupler, prognostic atmosphere and land, and ice and ocean data. The AGCM component is the Community Atmosphere Model (CAM5) version 5.1, using the finite volume dynamical core at the standard $0.9^{\circ} \times 1.25^{\circ}$ latitudelongitude resolution (f09_g16) and 30 vertical levels. The boundary and initial conditions for the control simulation were obtained from the CESM1 preindustrial control simulation and boundary conditions are fixed to that period; in particular, the sea surface temperature (SST) and sea ice are prescribed.

The control simulations with full Tibetan Plateau height ("Full Plateau"; Fig. 2a) is run for 55 years, with the last 50 years averaged to form the climatology. Since simulations are done using prescribed SST, 5 years is sufficient to spin up the model. Simulations reducing the topography over East Asia are also undertaken (see Table 1 for a summary of all simulation cases). In all cases, all land surface properties (apart from height) are kept to the same as the control simulation, as is the imposed SST. In the simulations that impose a reduced height to the plateau, the surface elevation of the region above 1500 m—which includes the Tibetan Plateau and the Himalayas—is set to a percentage of the difference between the actual height and 1500 m, with 100% being Full Plateau height and 0% being the topography limited to 1500 m. In all cases, the gravity wave drag parameterization is set to the Full Plateau case. The 0% simulation is hereafter referred to as the "No Plateau"

simulation (Fig. 2c), whereas the 100% simulation is the Full Plateau simulation. We also perform simulations increasing the plateau height to 25%, 50%, and 75% of its present-day height (Fig. 2b shows the 50% case). The "Thin Plateau" case sets the topography west of 100°E to No Plateau values, and uses the actual topography to the east of 100°E; this leaves the easternmost part of the plateau intact, but otherwise flattens it to 0% (Fig. 2d). All simulations are run for 55 years, with the last 50 years used to form the climatology.

We also perform a set of idealized simulations with the aquaplanet configuration of CAM5 (same model physics as the one used above) to investigate the basic ingredients of East Asian monsoon seasonality (section 6). To allow for a realistic seasonal migration of the westerlies, we include the seasonal cycle in the boundary conditions, in particular prescribing a seasonally varying but zonally symmetric SST. We derive this SST by zonally averaging the monthly climatological (1979– 2017) 1000-mb temperature field (1 mb = 1 hPa) from the NCEP-NCAR reanalysis (Kalnay et al. 1996), excluding temperatures over the region 20°-80°N, 0°-120°E; this was done to exclude Asia from the zonal average. The resulting temperature profile was smoothed spatially to eliminate sharp latitudinal variations in temperature. Finally, we set values below 0°C to zero. While this derivation of the aquaplanet SST is involved, the main purpose of the aquaplanet meridional SST profile is to provide boundary conditions that allows for a sufficiently realistic seasonal migration of the westerlies across the model-imposed plateau in the "idealized land + plateau" configuration (see below). For the base aquaplanet configuration, we turned off the land model and ice model and set the atmospheric distribution of ozone and aerosol to be globally uniform. With the next configuration ("idealized land-only"), we additionally introduce an idealized rectangular landmass of zero height across 0°-120°E and 20°-80°N to mimic a flat Asian-like continent. We make the imposed vegetation over the idealized land the same for a given latitude, in order to remove zonal variation. In CAM5, each land grid point has 16 different plant functional types, with each type given a fraction; the fractions over the 16 types sums to 1. In the idealized land, for each of the 16 plant functional types we impose the same fraction for a given latitude. This fraction is derived from zonally averaging, over 0°-120°E, the actual fraction in CAM5. For the idealized land + plateau configuration, we additionally introduce the Tibetan Plateau in the model land surface, and at the same latitude/longitude location as the real plateau, by setting surface geopotential across 25°-45°N and 65°-105°E to today's value. Elevations lower than 500 m in this region were set to zero. In the "idealized

TABLE 1. List of simulations and names used to refer to them.

Model configuration	Name	Comments
Realistic	Full Plateau (or 100%)	Present-day topography
	No Plateau	Topography of Tibetan
	(or 0%)	Plateau and Himalayas set to a maximum of 1500 m
	25%, 50%, 75% Plateau	Topography of Tibetan Plateau and Himalayas set to the specified percentage of the difference between 1500 m and actual height
	Thin Plateau	Actual topography east of 100°E, but set to No Plateau otherwise
Idealized	Aquaplanet	Zonally averaged SST
	Idealized land-only	Flat landmass 0°–120°E, 20°– 80°N imposed on the aqua- planet setup
	Idealized plateau-only	Tibetan Plateau (land 25°–45°N, 65°–105°E) imposed on aquaplanet setup
	Idealized land + plateau	Tibetan Plateau (topography 25°–45°N, 65°–105°E) imposed on the idealized land-only setup

plateau-only" simulation, we only impose land (including the topography) of the Tibetan Plateau region (25°–45°N, 65°–105°E); outside this region, fixed SSTs are imposed as in the base aquaplanet state. Each idealized run was integrated for 35 years, with the last 30 years used for analysis. Table 1 summarizes the set of idealized experiments and their configurations.

b. Simulated East Asian rainfall climatology

Figure 1b shows the precipitation in the Full Plateau simulation, highlighting the timing of the seasonal stages. The model clearly simulates the sequence of intraseasonal stages over land (north of $\sim 24^{\circ}$ N). Moreover, the model appears to simulate the differences in the rainfall type between stages (Figs. 3a,b). In observations, rainfall over East Asia over the spring, pre-meiyu, and mei-yu stages are predominantly from banded rainfall, whereas in midsummer rainfall is more local (nonbanded) (Day et al. 2018). Simulated rainfall in CAM5 is distinguished between "large-scale" and "convective," with the former being resolved by the model grid resolution, and the latter initiated by the model's convective parameterization. A loose comparison can be made between the banded rainfall in Day et al. (2018) and CAM5 simulated large-scale rainfall, under the assumption that banded rainfall is forced by large-scale uplift, and hence has a significant large-scale simulated rainfall component. As shown in Figs. 3a and 3b,

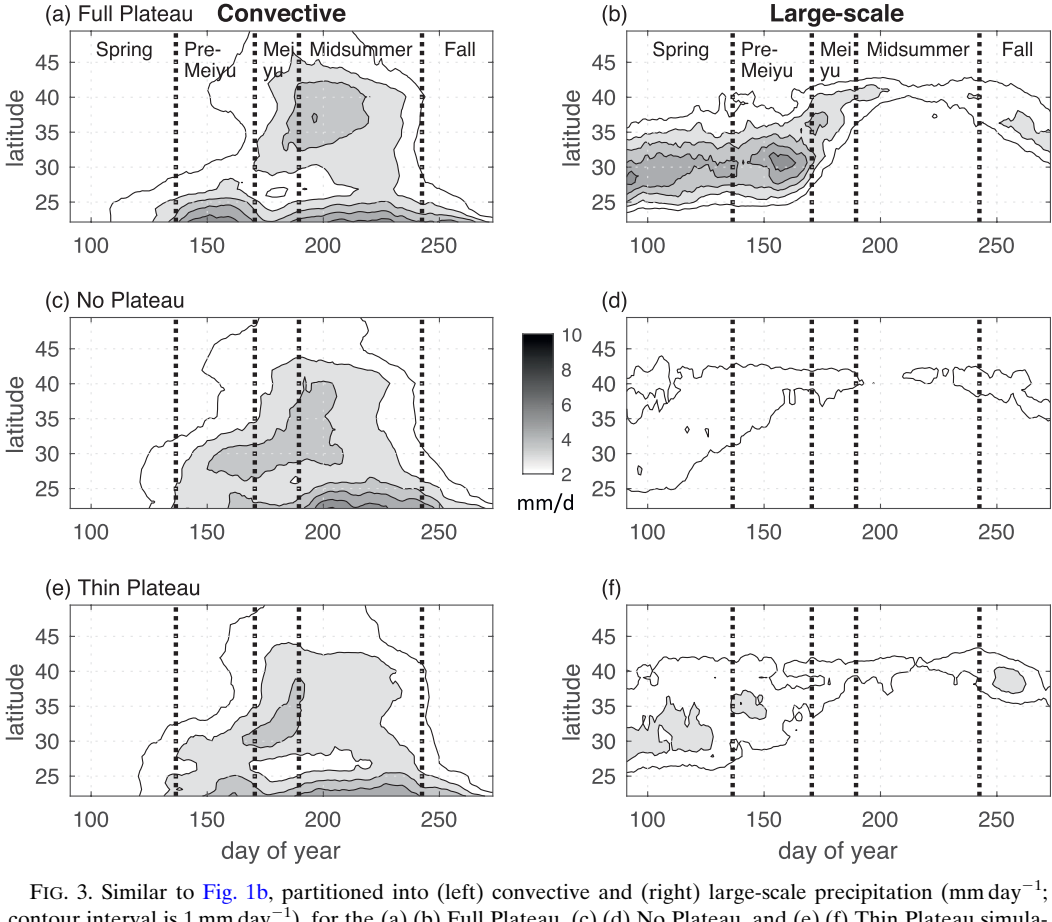


FIG. 3. Similar to Fig. 1b, partitioned into (left) convective and (right) large-scale precipitation (mm day⁻¹; contour interval is 1 mm day⁻¹), for the (a),(b) Full Plateau, (c),(d) No Plateau, and (e),(f) Thin Plateau simulations. In all cases, a 15-day running mean is applied prior to plotting; only contours of 2 mm day⁻¹ and above are drawn, and rainfall > 3 mm day⁻¹ is shaded. The vertical dashed lines in each panel indicate the boundaries separating the intraseasonal stages (spring, pre-mei-yu, mei-yu, midsummer, fall).

simulated precipitation during the spring stage is predominantly large-scale, consistent with the persistent and banded nature observed in the real world (Wu et al. 2007). Precipitation during the pre-mei-yu and mei-yu stages is also predominantly large-scale but with an increased convective contribution, again consistent with the banded nature of rainfall during those periods; simulated precipitation during midsummer is largely convective, consistent with the local nature of rainfall identified in Day et al. (2018).

However, there are differences in the timing and duration of the simulated intraseasonal stages from the observed. The rainfall over the South China Sea is not well simulated; this is partly a consequence of using prescribed SST rather than using a model with interactive SST (a CAM5 simulation coupled to a slab ocean model that we examined does simulate a more realistic climatology over the South China Sea; not shown). Since our focus is on the rainfall north of 24°N, we do not think that this unduly affects our results.

We obtain the timing of the seasonal stages objectively using a self-organizing maps (SOM) analysis of climatological rainfall; the methodology and its application to identification of the intraseasonal stages were first used by Kong et al. (2017). The premise is that the intraseasonal stages are quasi-stationary, and thus readily identifiable through SOM analysis of the daily rainfall climatology applied to the East Asian region. We follow a similar prescription to what is used in Kong et al. (2017) and refer the reader to that paper (section 2c) for details on the method. We perform the SOM analysis on daily rainfall with a 9-day running mean applied, and a rainfall domain of 20°-45°N, 110°-140°E. Table 2 shows the derived timing for the intraseasonal stages, using the SOM method. The timings of the simulated stages are compared to a similar SOM analysis but from an observed daily gridded rainfall climatology using the APHRODITE dataset (APHRO_MA_0.25deg_V1003R1; Yatagai et al. 2012) averaged over 1951-2007 and as reported in Chiang et al. (2017). The two timings are

TABLE 2. Timing of the intraseasonal stages from observations and in the Full Plateau simulation. The timing of the observed stages comes from Chiang et al. (2017) applying the self-organizing map (SOM) method to a observed gridded rainfall climatology (with 9-day running mean applied), whereas the timing for the Full Plateau simulation is from SOM analysis of simulated daily rainfall, also with 9-day running mean applied (see text for details). The timings generally coincide. Note also that different names have been used in the literature for the various intraseasonal stages; in particular, the midsummer stage is also commonly known as the post-mei-yu. The names we use for the stages here follow from our previous papers (Chiang et al. 2015; 2017; Kong et al. 2017).

Intraseasonal stage	Observed rainfall (following Chiang et al. 2017)	Full Plateau simulation
Pre-mei-yu	27 May-24 Jun	16 May-18 Jun
Mei-yu	25 Jun-18 Jul	19 Jun-8 Jul
Midsummer	19 Jul-5 Sep	9 Jul-31 Aug

comparable except for the termination of the mei-yu stage, which occurs in mid-July in observations (17 July), but early July (7 July) in the model; this results in a significantly shorter simulated mei-yu stage, and a longer midsummer stage. In observations, an earlier mei-yu termination occurs about two weeks early in one phase of the "tripole" mode of interannual variability in the July–August East Asian rainfall (Chiang et al. 2017); in fact, the simulated rainfall climatology (Fig. 1b) resembles the "early mei-yu" climatology (see Fig. 3a of Chiang et al. 2017). Thus, this earlier termination is realized in some years in the observed rainfall record and is related to an earlier northward migration of the westerlies (Chiang et al. 2017).

The position of the simulated westerlies relative to the plateau for each stage is shown in Fig. 4, bottom row. There is a good resemblance both in terms of the structure and meridional positioning of the westerlies for each stage compared to NCEP reanalysis (Fig. 4, top row); the core of the westerlies straddle the northern edge of the plateau (\sim 40°N) during the mei-yu, but is to the south of this during the pre-mei-yu and to the north of this during midsummer. This resemblance is notable given that the exact timing of the simulated stages differs from the observed; in plotting the simulated westerlies using the observed timing of the stages, clear differences between the observed and simulated westerlies are apparent (not shown). This result is consistent with the hypothesis that the intraseasonal stages are determined by the configuration of the westerlies relative to the plateau.

3. Simulations removing the Tibetan Plateau

A set of simulations systematically altering the elevation of the Tibetan Plateau is done to illustrate the direct effect of the plateau on the East Asian summer monsoon. While there have been many modeling studies examining the effects of reducing the plateau (e.g., Abe et al. 2003; Chen and Bordoni 2014; Kitoh 2004) none have explicitly focused on the origins of seasonal stages over East Asia. When the plateau is flattened to 0% (the No Plateau simulation), the seasonal transitions disappear, leaving instead a single summer rainfall season with an onset around the start of the pre-mei-yu stage and termination around the end of the midsummer stage (Fig. 1c). Moreover, the rainfall is mostly convective, as opposed to the Full Plateau case where there is a mix of large-scale and convective rainfall (Figs. 3c,d compared to Figs. 3a,b). The rainfall in the No Plateau case is also meridionally uniformly distributed across southeastern to northeastern China, unlike the Full Plateau case where the total rainfall is more concentrated north of ~35°N (Figs. 1b,c). The major difference between the two cases comes from the large-scale rainfall (cf. Figs. 3b,d), as the convective rainfall is qualitatively similar between the two cases (cf. Figs. 3a,c).

As the plateau height is progressively increased, the seasonal characteristics of today's East Asian monsoon emerge (Figs. 5a-d). It clearly shows the pattern of rainfall systematically evolving from the No Plateau case (Fig. 5e)—with no distinct intraseasonal stages—to the Full Plateau case with the intraseasonal stages (Fig. 5a). Three features are particularly noticeable. First, for higher plateau heights the rainfall during the pre-mei-yu through midsummer stages is meridionally concentrated, whereas for low plateau heights the rainfall is more uniformly spread across latitudes between southeastern and northeastern China; this meridional concentration, and latitudinal migration, is what gives the Full Plateau rainfall its intraseasonal character. Second, the rainfall over the spring, pre-mei-yu, and mei-yu stages increase significantly as the plateau height is increased, and the increase is almost entirely due to the increase in large-scale rainfall (cf. Figs. 3b,d). Third, the northward migration of rainfall during the mei-yu period emerges with increasing plateau elevation, mainly due to the increasing importance of large-scale rainfall, which migrates northward during this period. The increasing contribution of large-scale rainfall is consistent with the large-scale circulation and uplift downstream forced by the thermal and mechanical forcing by the plateau (e.g., Liu et al. 2007). The overall intensity of rainfall also increases with increasing plateau thickness; this feature has been noted previously (e.g., Abe et al. 2003).

We apply a vertically integrated moisture budget analysis to each of the stages to reveal the underlying cause of the precipitation changes between the Full and No Plateau cases. Following Eq. (3) of Chiang et al. (2019), the budget is written as follows:

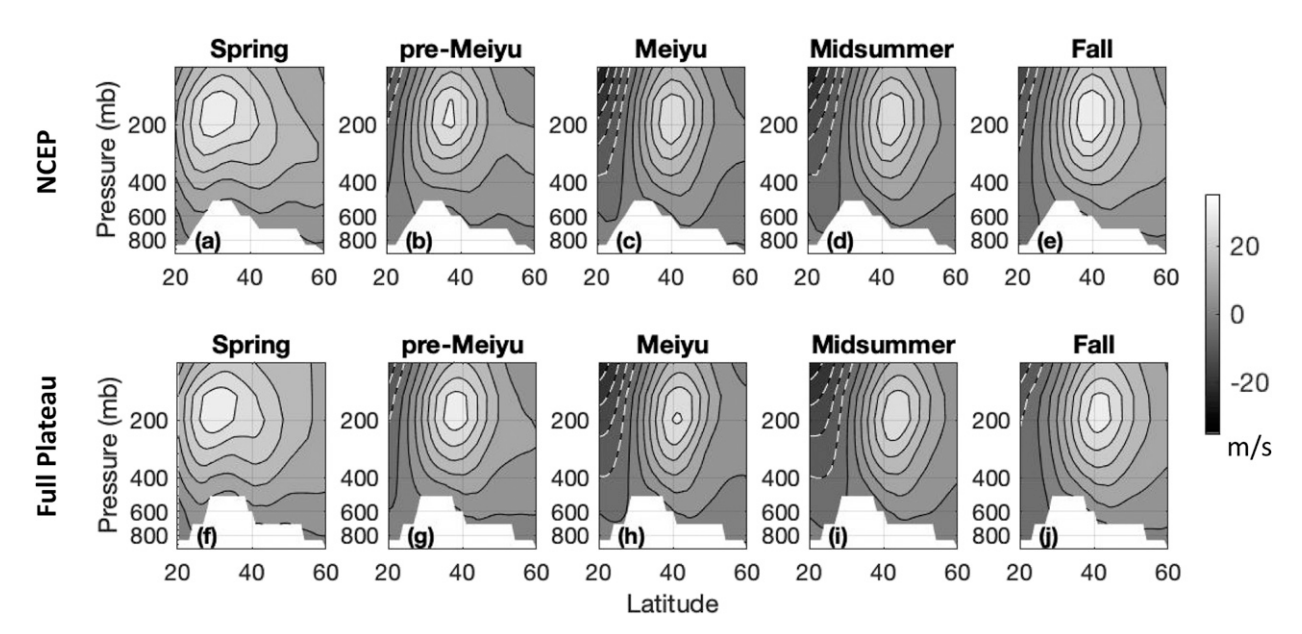


FIG. 4. (a)—(e) Observed (NCEP reanalysis) climatological zonal mean zonal winds straddling the plateau, averaged over 60°–125°E, for each of the five stages. The timings are based on the identification in Chiang et al. (2017), summarized in Table 2. The climatology is taken over years 1951–2007 to coincide with the rainfall climatology in Fig. 1a. The contour interval is 5 m s⁻¹, and white dashed lines are negative contours. The data for this figure are the same as Figs. 4a–e of Chiang et al. (2017). (f)–(j) As in (a)–(e), but for the model simulation, and using the SOM-derived timings summarized in Table 2. The observed and simulated winds are qualitatively similar (in particular the meridional position of the maximum wind), despite the fact that the timing of the simulated stages differ slightly from those observed; this supports the hypothesis that the stages are determined by the meridional position of the westerlies relative to the plateau.

$$\delta(P - E) = -\delta \langle \nabla. (\mathbf{v}q) \rangle = -\langle \nabla. [\mathbf{v}(\delta q)] \rangle - \langle \nabla. [(\delta \mathbf{v})q] \rangle$$

$$-\langle \nabla. [(\delta \mathbf{v})(\delta q)] \rangle - \delta(\text{tr}),$$
(d)
(1)

where P-E is evaporation minus precipitation, \mathbf{v} is the horizontal wind, q the specific humidity, tr the transient term, and $\langle \cdot \rangle$ denotes the vertical integral taken from the surface to 100 mb; δ is the difference between the Full and No Plateau (the former minus the latter). The difference in P-E equals the change in the vertically integrated moisture flux convergence [term (a)]. The latter in turn can be broken up into contributions from the change to the specific humidity [thermodynamic term; term (b)], horizontal wind [dynamic term; term (c)], the cross-perturbation term [term (d)], and transients [term (e)]. Daily values are used in the calculation of each budget term and averaged over the days occupied by the intraseasonal stage (using the timings in Table 2).

Figure 6 shows terms (a)–(e) of Eq. (1) for the premei-yu stage [note that Figs. 6a–e correspond to terms (a)–(e) of Eq. (1), respectively]. The emergence of the rainband with the Full Plateau is clearly seen in term (a), and the budget analysis shows that this is primarily a consequence of the change in the horizontal winds (Fig. 6c). The change associated with specific humidity

(Fig. 6b) and cross-perturbation term (Fig. 6d) are small by comparison. The transient term (Fig. 6e) acts to damp the contribution from the horizontal wind changes. Decomposing the horizontal wind change into its zonal (Fig. 6f) and meridional (Fig. 6g) components shows that the change to the meridional winds is responsible for the emergence of the rainband, with the zonal wind contribution acting in opposition. Finally, breaking the meridional wind contribution into mass convergence (Fig. 6h) and advection (Fig. 6i) shows that the change in the meridional wind convergence explains virtually all of it.

Thus, the moisture budget analysis shows that it is the change to the meridional wind convergence that produces the rainband in the pre-mei-yu stage. This is consistent with the findings of Chen and Bordoni (2014) comparing simulation with and without a Tibetan Plateau, but using the vertically integrated moist static energy budget. Repeating this analysis for the mei-yu (see Fig. S1 in the online supplemental material) and mid-summer (Fig. S2) stages similarly shows that the change in the rainfall pattern over East Asia arises through changes in the meridional flow, and specifically from meridional wind convergence. Thus, it is the meridional wind changes that are responsible for the bringing about the intraseasonal stages. In the next two sections, we argue that the extratropical northerlies introduced by

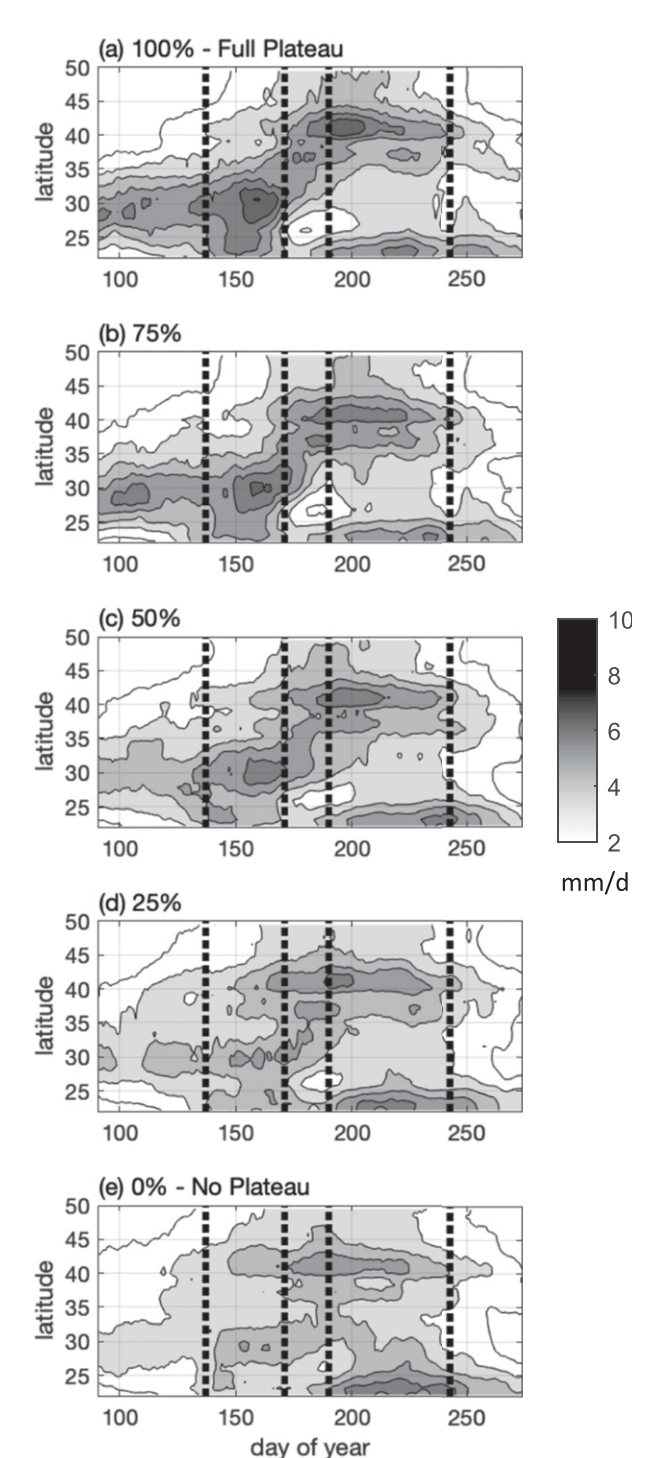


FIG. 5. Emergence of the seasonal stages in the East Asian summer monsoon with plateau thickness. Simulated total rainfall (mm day⁻¹; contour interval is 1 mm day⁻¹) zonally averaged over 110°–125°E for (a) the Full Plateau simulation and the plateau at (b) 75%, (c) 50%, (d) 25%, and (e) 0% (i.e., No Plateau). A 15-day running mean is applied prior to plotting. Only contours 2 mm day⁻¹ and above are drawn; regions of heavier rainfall (>3 mm day⁻¹) are shaded. The vertical dashed lines indicate the boundaries separating the intraseasonal stages (spring, pre-mei-yu, mei-yu, midsummer, fall). Note that unlike Fig. 1b, here we take the zonal average from 110°–125°E, and ocean points are included.

the presence of the Tibetan Plateau play the key dynamical role.

4. The downstream extratropical northerlies and the intraseasonal stages

The introduction of the Tibetan Plateau thus leads to the emergence of the intraseasonal stages. Following on from Kong and Chiang (2019), we argue that the key circulation feature that leads to this emergence are the extratropical upper and midtropospheric northerlies that appear downstream of the plateau, centered around northeastern China. We elaborate in section 5 the dynamical reasons why the northerlies are important. Here, we first show that these northerlies are a direct result of the presence of the plateau, and that its evolution across the summer months is consistent with the rainfall intraseasonal rainfall stages.

The tropospheric northerlies introduced by the presence of the plateau, centered over northeastern China, are shown in Figs. 7 and 8a. They are prominent during the spring and pre-mei-yu stages (Figs. 7a,b), but weaken and retract westward toward the plateau during the meiyu (Fig. 7c). By the midsummer (Fig. 7d), the northerlies have retracted westward to the plateau longitudes, and the northerly meridional flow over northeastern China is replaced by tropospheric southerlies. The northerlies induced by the plateau bring drier extratropical air southward to central eastern China, where it meets up with warm and moist air from the tropics (Fig. 8b, shaded). During the spring and pre-mei-yu, these two opposing flows meet over central eastern China, consistent with the rainfall being located there (Fig. 8a) With the start of the mei-yu stage however, the northerlies weaken and the latitude where the two flows meet shifts northward (Fig. 8a), in sync with the northward migration of the rainband. With mei-yu termination, the northerlies essentially disappear and the lower tropospheric monsoonal southerlies—which were restricted to southeastern China prior to mei-yu termination—now penetrate all the way into northeastern China, and the midsummer rainfall locates itself there (Fig. 8a). The extratropical northerlies re-establish at the end of the midsummer and beginning of the fall stage.

This covariation between the rainfall stages and the extratropical northerlies suggests that the strength of the midtropospheric northerlies over northern China is key to understanding the intraseasonal evolution, specifically the northward migration of the mei-yu and transition to the midsummer stage. As the westerlies shift northward relative to the Tibetan Plateau, the extratropical northerlies become weaker until the westerlies

are no longer significantly influenced by the plateau. On the other hand, as summer progresses the tropical southerly monsoonal flow increases, as a result of both land-ocean thermal contrast increases (Liang et al. 2005) and diabatic heating associated with an intensifying South Asian monsoon (Liu et al. 2007; Wu et al. 2012a). The lower and midtropospheric southerly flow is actually strongest in the mei-yu stage, but we will argue that this additional strengthening is a positive feedback to the diabatic heating caused by the mei-yu rainband (see section 5).

We explicitly test the role of the plateau in generating the northerlies with an idealized simulation. Mechanically driven stationary eddies are produced by mountain ranges with significant zonal width like the Tibetan Plateau or the Rockies (Bolin 1950); the Andes on the other hand are thought to be too narrow to produce appreciable stationary eddy circulations, at least through mechanical effects (Lenters et al. 1995). The presence of the plateau also introduces diabatic heating effects, directly through sensible heating over the plateau (Wu et al. 2012b) and indirectly through inducing the South Asian monsoon (Boos and Kuang 2010);¹ the associated heating drives stationary eddy circulations across Asia (Liu et al. 2007). These insights motivate us to perform an idealized Thin Plateau simulation where we terminate the Tibetan Plateau at 100°E, so that the topography to the west of the plateau resembles the No Plateau simulation, but the topography remains the same to the east (Fig. 2d). In principle, the plateau topography in this simulation should be too narrow longitudinally to produce significant midlatitude stationary eddies, or to significantly alter the thermal forcing, as compared to the No Plateau case.

Consistent with our hypothesis, precipitation in the Thin Plateau simulation (Fig. 1d), does not reproduce the intraseasonal stages simulated in the Full Plateau simulation (Fig. 1a); instead, the rainfall looks qualitatively more like the No Plateau case (Fig. 1c). As with the No Plateau case, large-scale rainfall in the pre-meiyu through midsummer periods is considerably reduced (Fig. 3f). Convective rainfall starts during the pre-mei-yu

periods over southeastern China and expands to the north during what would be the mei-yu and midsummer periods (Fig. 3e). Taken together, these results suggest that the stationary eddy influence of the plateau—both mechanical and thermal—is responsible for a significant fraction of the pre-mei-yu and mei-yu rains, as well as the northward migration of the mei-yu rainband. In support of the latter interpretation, the Thin Plateau simulation lacks the extratropical northerly response downstream of the plateau (Figs. 7e–h); furthermore, the meridional position of the upper-level westerlies does not change significantly between the No Plateau runs and Thin Plateau simulations (not shown).

5. Interaction between the monsoonal circulation and extratropical northerlies

We posit two distinct atmospheric circulations that are responsible for East Asian monsoon seasonality. The first circulation is the southerly monsoonal flow driven by land-ocean contrasts typical of a subtropical monsoon system (specifically the pressure difference between the Asian continent and the western Pacific subtropical high), and stationary eddy circulations generated by the plateau directly through either mechanical or thermal forcing, or indirectly via South Asian monsoon heating. The second circulation—and what makes the East Asian monsoon distinct—is the extratropical northerly influence downstream of the Tibetan Plateau due to the westerlies impinging on the plateau. The subtropical monsoon circulation is obvious for understanding the East Asian monsoon seasonality, but the focus on the extratropical northerlies is less so. Motivation for doing so comes from two recent studies. Chen and Bordoni (2014) found from a moist static energy budget analysis that the moist enthalpy advection by the meridional stationary eddy circulation was key for energetically sustaining the mei-yu rainband; moreover, the removal of the plateau changes the stationary enthalpy flux primarily through altering the meridional stationary eddy circulation. This result is consistent with our own simulations in removing the plateau. Furthermore (and as highlighted in section 1), Kong and Chiang (2019) showed that mei-yu termination is causally linked to the disappearance of the northerlies, through the latter's effect on the meridional contrast of equivalent potential temperature across the mei-yu front, and on the lowertropospheric horizontal wind convergence. Taken together, these studies imply that if the strength of the extratropical northerlies change as summer progresses, it will have a direct impact on the seasonal evolution of East Asian rainfall.

¹ There is a current debate on the role of the Tibetan Plateau in the formation of the South Asian summer monsoon, whether it is induced by sensible heating over the plateau and over the southern slope and Himalayas (Wu et al. 2012b), or through the insulation effect by plateau topography (Boos and Kuang 2010, 2013). South Asian monsoon heating matters to our analysis only insofar as it drives stationary eddy circulations and in particular tropical southerlies over the East Asian monsoon region; the exact origin of the South Asian heating is not material for our analysis, and we stay neutral in this debate.



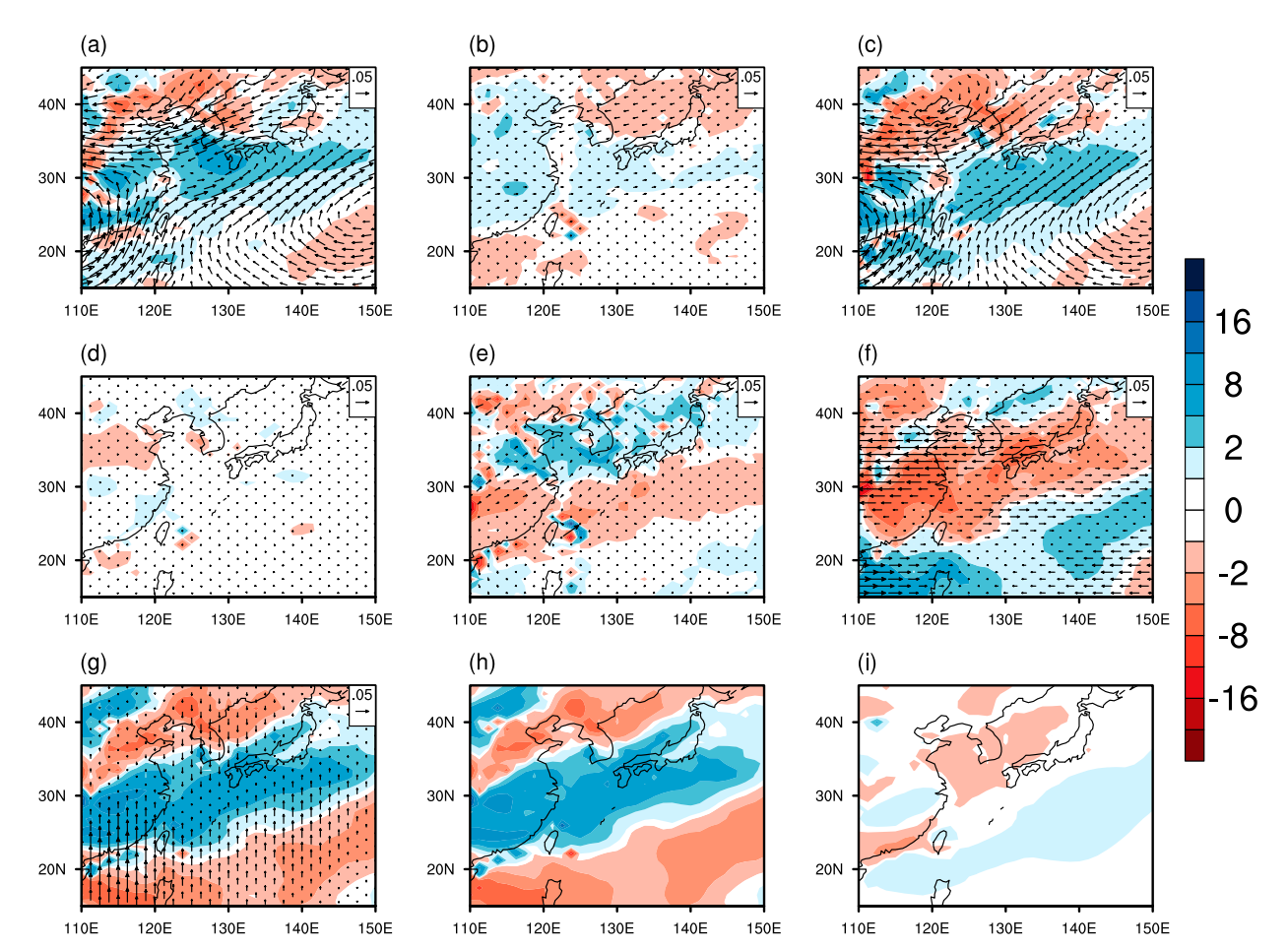


FIG. 6. Vertically integrated moisture budget analysis of the change in P-E between the Full and No Plateau simulations. The terms are (a) $-\delta\langle\nabla\cdot(\mathbf{v}q)\rangle$, the full moisture flux convergence; (b) $-\langle\nabla\cdot[\mathbf{v}(\delta q)]\rangle$, the contribution from change to specific humidity; (c) $-\langle\nabla\cdot[(\delta\mathbf{v})(\delta q)]\rangle$, the contribution from the crossperturbation term; and (e) $-\delta(\mathrm{tr})$, the contribution from change to the transient term. (f),(g) The contributions from the change to the zonal and meridional winds, respectively. The meridional wind contribution is further broken into (h) $-\langle qd_y\delta v\rangle$, the contribution from meridional wind convergence, and (i) $-\langle\delta vd_yq\rangle$, the contribution from meridional advection. The color scale is in mm day $^{-1}$, and the reference vector $0.05\,\mathrm{m}^2\,\mathrm{s}^{-1}$.

We illustrate the two distinct flows and their evolution through cross sections of the observed meridional wind just downstream of the Tibetan Plateau over eastern China (110°–125°E) (Figs. 9a–e). During spring (Fig. 9a), the meridional winds possess a barotropic structure with southerlies south of 30°N and northerlies to the north; this resembles the reconvergence of the split jet downstream of the plateau, and indeed the zonal winds over the plateau shows the characteristics of a split jet during this time (Fig. 4a). The extratropical northerlies persist in the pre-mei-yu stage (Fig. 9b), but the tropical southerlies change from a more barotropic structure in spring to a more baroclinic structure with strong southerlies in the middle and lower troposphere. We interpret the absence of the barotropic southerlies to the demise of the split jet as the westerlies shift away from the southern part of the plateau (Fig. 2b). The lower tropospheric southerlies are due to the strengthening of the low-level monsoonal flow as summer progresses and to the diabatic heating caused by the rainband itself (more on this later). The convergence of the lower-tropospheric tropical southerlies and extratropical northerlies results in a dynamically induced humidity front around 31°N that determines the location of the rainband.

During the mei-yu stage (Fig. 9c), the extratropical northerlies weaken while the lower and midtropospheric tropical southerlies strengthen; as a result, the humidity front shifts farther northward to around 33°N, leading to the northward migration of the mei-yu rainband. By the midsummer stage (Fig. 9d), the extratropical northerlies disappear as the westerlies move north of the plateau (Figs. 4d,i); what remains is a lower-tropospheric southerly monsoonal flow that penetrates into northern China and brings moisture there (cf. Fig. 8b). In the fall stage,

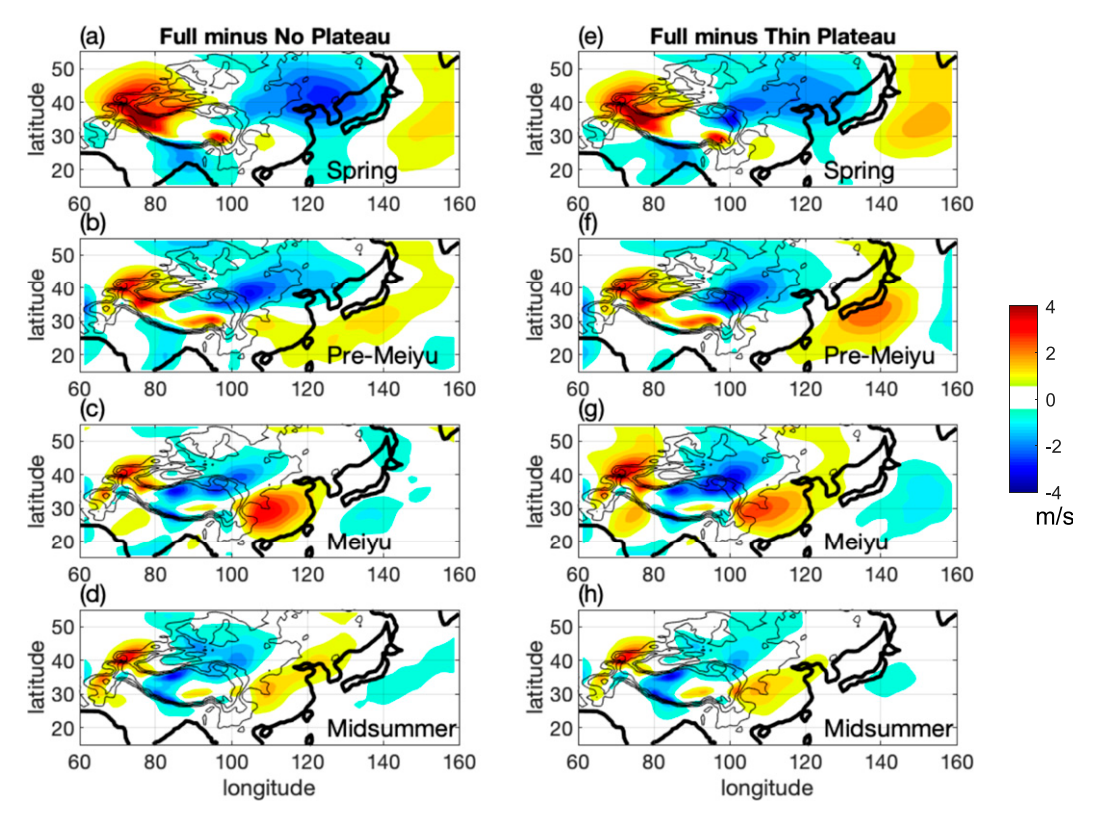


FIG. 7. Change to the 500-mb meridional wind $(m s^{-1})$, Full Plateau minus No Plateau, averaged over the (a) spring, (b) pre-mei-yu, (c) mei-yu, and (d) midsummer stages. (e)–(h) As in (a)–(d), but for Full Plateau minus Thin Plateau. Compared to the influence of the Full Plateau, the Thin Plateau has relatively little influence on the meridional circulation.

the westerlies move back to the north of the plateau, and the extratropical northerlies reappear (Fig. 9e).

We support our interpretation above by examining the difference between the Full Plateau and No Plateau simulations; the circulation in the latter experiment is assumed to be from the monsoonal influence only. First note that the Full Plateau simulations exhibit intraseasonal behavior in meridional wind and specific humidity that resembles the observed (contrast Figs. 9f-j with Figs. 9a-e), giving us the confidence to use these simulations; the one notable exception being the tropical southerlies during spring, which lacks a pronounced barotropic structure. By contrast, the same fields for the No Plateau simulation (Figs. 9k-o) show a very different structure, with low-level monsoonal southerlies during the pre-mei-yu, mei-yu, and midsummer stages, as would be expected of a monsoon circulation; the northerlies occupy the upper troposphere and are centered in the subtropics, as would be expected of the return flow of a Hadley-like circulation.

The difference between the Full Plateau and No Plateau simulations reveals the contribution of the plateau to the meridional circulation, as shown in Figs. 9p-t.

For the spring and pre-mei-yu periods (Figs. 9p,q), the plateau influence on the meridional winds is consistent with the interpretation we provide above, namely (i) part of the lower-tropospheric southerly flow is monsoonal in origin, independent of the plateau; and (ii) the barotropic extratropical northerlies are a consequence of the plateau, as are the lower-midtropospheric tropical southerlies. They also show that the plateau influence weakens during the mei-yu² (Fig. 9r) and recedes in midsummer (Fig. 9s),

²Note that the No Plateau simulation does not completely flatten the plateau, but rather limits plateau topography to 1500 m, so there are still orographic effects on the circulation. This is especially relevant for the comparison between the Full and No Plateau for the mei-yu case, as the westerlies in the Full Plateau simulation encounters the northern edge of the plateau, which is lower than the height at the center of the plateau (Fig. 4h). As a result, the distinction between the Full and No Plateau case for the mei-yu is not as pronounced as for the spring and pre-mei-yu stages, in terms of the orographic influence on the westerlies. This explains the relative lack of anomalous northerlies in Fig. 9r. We ran another simulation limiting the height of the Asian topography (20°–60°N, 60°–125°E) to 500 m (not shown), and the results support this interpretation.

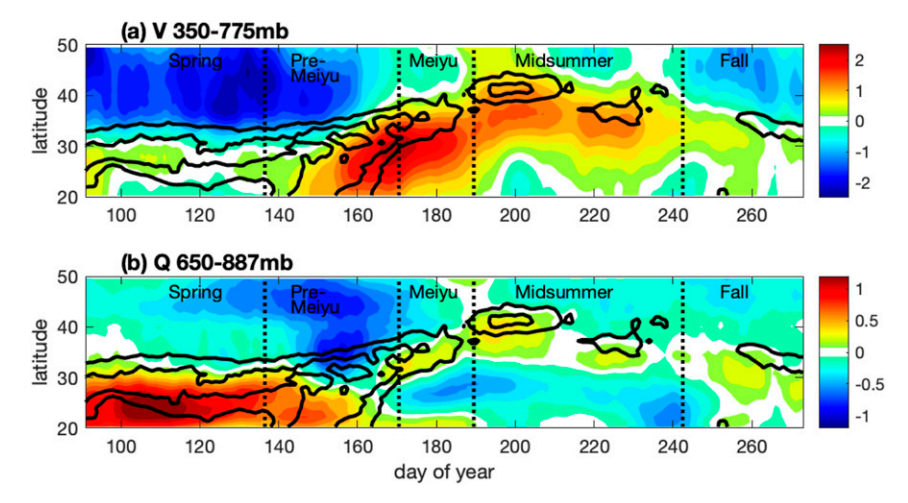


FIG. 8. Change to the (a) tropospheric meridional winds (mass-weighted over 350–775 mb; m s⁻¹) and (b) lower tropospheric specific humidity (mass-weighted over 650–887 mb; g kg⁻¹) over East Asia from the introduction of the plateau. The black contours in both panels show the corresponding change in the precipitation, at contour intervals of 1, 2, and 3 mm day⁻¹. Plots are Full Plateau minus No Plateau Hovmöller plots, zonally averaged over 110°–125°E. Daily data were used, and a 15-day running mean applied prior to plotting. The dashed lines demarcate, from left to right, the beginning of the pre-mei-yu, mei-yu, midsummer, and fall stages.

consistent with the picture that the westerlies have shifted north of the plateau during this time. The anomalous northerlies reappear in the fall (Fig. 9t), consistent with the westerlies migrating southward toward the plateau.

The difference in the specific humidity between the Full and No Plateau simulations (Figs. 9p-t) also reveals the dynamical nature of the humidity front, and the role of the plateau in setting this up. The lower tropospheric specific humidity increases where the tropical southerlies are present, and decreases where the extratropical northerlies are present; and in particular the humidity increases the most at the northern edge of the southerlies (contrast Fig. 9g with Fig. 9q, and Fig. 9h with Fig. 9r). We conclude that the plateau plays a decisive role in establishing the lower-tropospheric meridional convergence and position of the humidity front from the spring through the mei-yu stage, consistent with the results from the moisture budget analysis in section 3 and Fig. 6.

The question remains as to where the tropical southerlies—apart from the lower-tropospheric monsoonal contribution—originate. We interpret those southerlies to result from two contributions: 1) from the local response to diabatic heating induced by the rainband convection, occurring just south of the humidity front, and 2) from remote diabatic heating over South Asia. For the latter, Liu et al. (2007) and Wu et al. (2012b) show that South Asian diabatic heating drives southerly flow into eastern China. For the former, diabatic heating associated with the rainband leads to vertical motion peaking in the midtroposphere (Figs. 10a–e); by Sverdrup

balance, the stretching of the atmospheric column below the vertical motion peak must be balanced by a southerly flow (Liu et al. 2001; Rodwell and Hoskins 2001; Wu et al. 2009); this approximately explains the tropical southerlies, at least in the vicinity of the vertical motion. The Full Plateau simulations provide a remarkably similar picture to the observations (cf. Figs. 10a—e with Figs. 10f—j). Thus, the tropical southerlies just south of the humidity front, during the pre-mei-yu and mei-yu, is a feedback response to the convective heating, and the flow in turn maintains the convection through the import of tropical moisture.

In summary, the intraseasonal evolution of the East Asian monsoon results from an interaction between the tropical southerly monsoonal flow and the extratropical northerly flow. The extratropical northerlies limit the northward penetration of the monsoonal flow, resulting in a humidity front and rainfall at the convergence between them in the lower troposphere. The resulting diabatic heating leads to a strengthening of the tropical lower and midtropospheric southerlies, reinforcing the moisture transport, convergence, and humidity front and supporting further convection. When the mei-yu commences, the monsoonal flow strengthens while the extratropical northerly flow weakens, resulting in a northward migration of the humidity front and rainband. When the westerlies shift north of the plateau during the midsummer, the extratropical northerlies disappear and only the monsoonal low-level southerlies remain; as a result, the rainband disappears, and without



Downloaded from http://journals.ametsoc.org/jcil/article-pdf/33/18/7945/4990290/jcild190888.pdf by guest on 17 August 2020

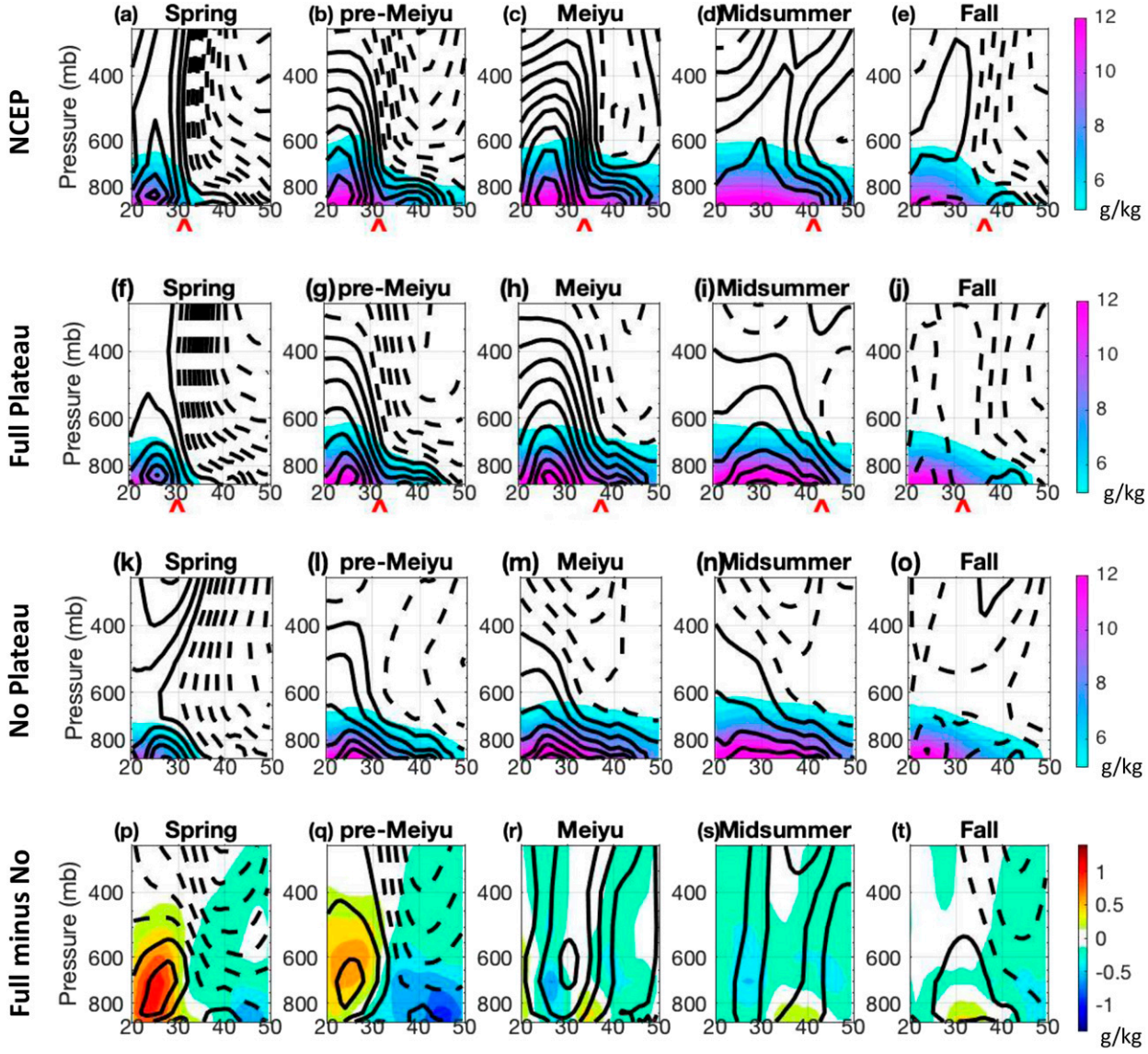


FIG. 9. Climatology of meridional wind (m s $^{-1}$; contours) and specific humidity (g kg $^{-1}$; color scale on right) zonally averaged over 110°–125°E, for each intraseasonal stage. (a)–(e) NCEP reanalysis averaged over 1961–90 (years correspond to Fig. 3), (f)–(j) the Full Plateau simulation, (k)–(o) the No Plateau simulation, and (p)–(t) the Full minus No Plateau simulation. The red chevron at the base of (a)–(j) indicates the location of maximum meridional specific humidity gradient at 850 mb, as an indicator of the humidity front. The contour interval is $0.6 \, \mathrm{m \, s}^{-1}$ for all panels, and dashed lines are negative contours; the first negative contour is $-0.3 \, \mathrm{m \, s}^{-1}$, and the first positive contour is $+0.3 \, \mathrm{m \, s}^{-1}$.

Latitude

the northerlies to constrain the flow, the monsoon penetrates to northeastern China.

6. The basic ingredients of East Asian monsoon seasonality

The separate and contrasting roles of the low-level monsoonal flow and stationary eddy circulation driven by the Tibetan Plateau suggests two basic ingredients of East Asian monsoon seasonality: 1) a landmass covering the subtropics and midlatitudes that provides a land—ocean contrast, specifically leading to a subtropical high to the east that drives a southerly flow into the eastern part of the continent; and 2) a plateau of sufficient longitudinal and latitudinal width to the west of the eastern landmass, and located sufficiently north that the core of the westerlies impinges on it during the winter and spring months and migrates to the north of it during the

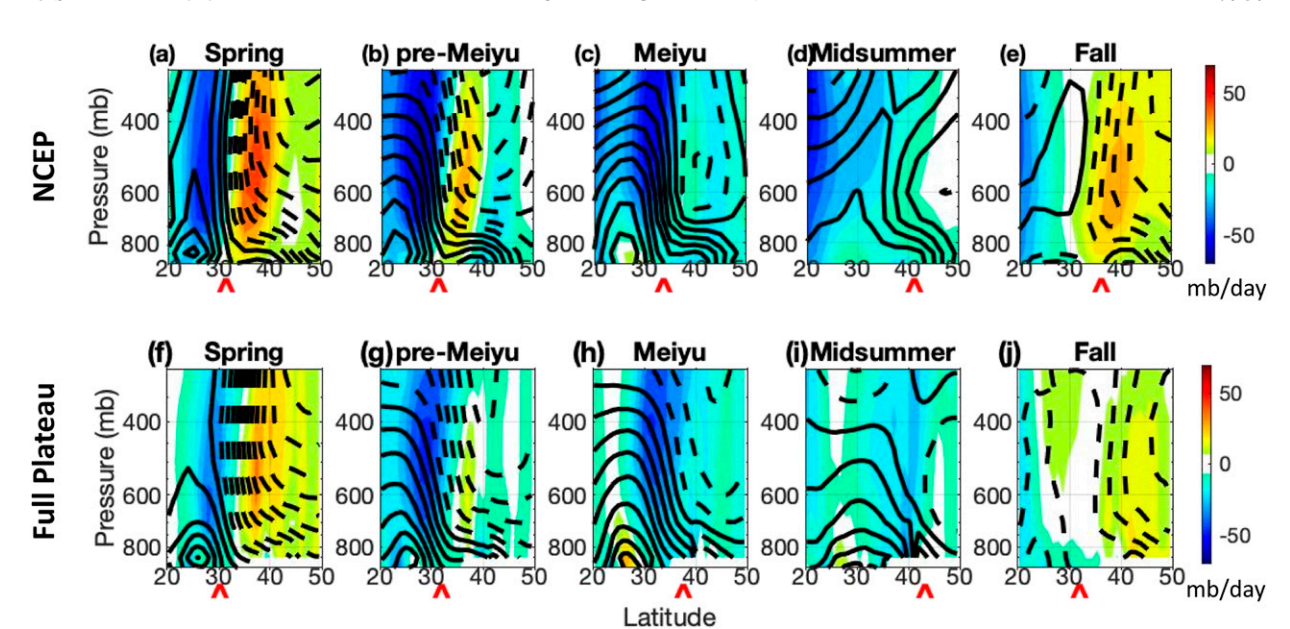


Fig. 10. Meridional winds (m s⁻¹; contours) and pressure vertical velocity (mb day⁻¹; shaded) zonally averaged over East Asia 110° – 125° E, for each of the intraseasonal stages, from (a)–(e) NCEP reanalysis and (f)–(j) the Full Plateau simulation. The red chevrons indicate the location of the humidity front as calculated in Fig. 8; note that for the spring, pre-mei-yu, and mei-yu stages, the humidity front is located at the northern edge of the peak uplift region. The contour interval is $0.6 \, \text{m s}^{-1}$ for all panels, and dashed lines are negative contours; the first negative contour is $-0.3 \, \text{m s}^{-1}$, and the first positive contour is $+0.3 \, \text{m s}^{-1}$.

summer, and furthermore allows for the South Asian monsoon heating to occur in the summer.

To test this idea, we produce a set of simulations imposing an idealized landmass and plateau in an otherwise featureless aquaplanet with imposed SST. Section 2a describes the details of the simulations, but the essential aspects are that the imposed SST is zonally symmetric and seasonally varying, and the insolation is also prescribed to be seasonally varying; these boundary conditions allow for a reasonable realistic Northern Hemisphere westerlies including its seasonal migration. The landmass is idealized (rectangular in latitude-longitude space) and is sized and positioned to roughly represent the Asian landmass, and the plateau is the actual Tibetan Plateau as represented in CAM5. Our control simulation is the base aquaplanet with neither landmass nor plateau. We then undertake three additional simulations: 1) land but no plateau (the idealized landonly run; 2) land and plateau (the idealized land + plateau run); and 3) aquaplanet with imposed SST as before, but including an embedded plateau (the idealized plateau-only run).

The seasonal rainfall associated with the idealized land-only simulation is shown in Fig. 11a. As with the No Plateau simulation (Fig. 1c), it produces only one rainy season in the summer and almost entirely from convective rainfall (figure not shown). The rainfall is relatively weak, in particular north of 30°N (note that the

idealized land extends as far south as 20°N here, whereas the coastline of southeastern China is ~24°N). The simulation results here are consistent with the modeling results of Liang et al. (2005) with a similar idealized land setup. With the addition of a Tibetan-like plateau on top of the subtropical land, intraseasonal rainfall stages emerge (Fig. 11b) that is similar to those in the Full Plateau simulation (cf. Figs. 11b and 1b), with a northward migration during the mei-yu-like stage and a northward-displaced rainfall maximum in the midsummer-like stage. The rainfall is also significantly more intense over the spring and summer months, in large part to the contribution of large-scale rainfall that is absent in the idealized land-only simulation.

The introduction of the plateau in the idealized land + plateau simulation produces seasonally evolving extratropical northerlies, similar to the Full Plateau case when contrasted against the No Plateau simulation (Figs. 7a,b). We use the 500-mb meridional wind to identify the timings of the mei-yu and midsummer-like stages in the idealized land + plateau simulation and denoted by the vertical dashed line in Fig. 11. The weakening and northward retreat of the extratropical northerlies occurring around pentad 32 (early June) marks the start of the mei-yu-like period, and the disappearance of the northerlies around pentad 40 (mid-July) marks the start of the midsummer-like period; this period ends around pentad 45 (early August).

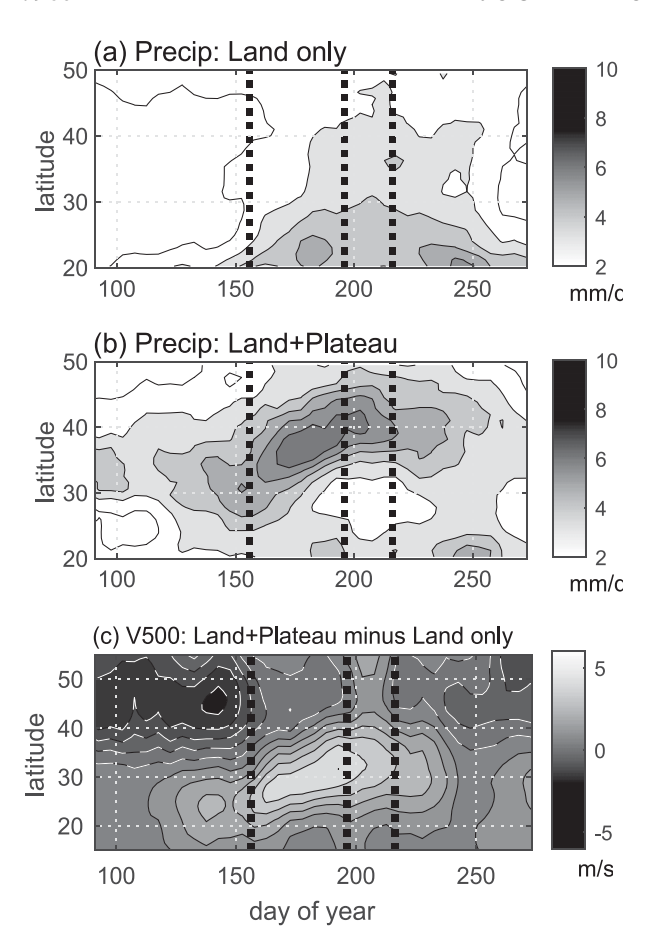


FIG. 11. Hovmöller of rainfall zonally averaged over 110°–120°E for the (a) idealized land-only and (b) idealized land + plateau simulation. A 15-day average running mean is applied prior to plotting. The contour interval is 1 mm day⁻¹, and only contours above 2 mm day⁻¹ are plotted. (c). Hovmöller of difference (idealized land + plateau minus land-only) in the 110°–120°E zonal mean of 500-mb meridional wind (contour interval is 1 m s⁻¹; white dashed contours are negative). The black dashed lines correspond to the start of pentads 32, 40, and 44, respectively, corresponding to the start of the mei-yu, midsummer, and fall-like stages.

We contrast further the difference between the idealized land-only and idealized land + plateau simulations for the mei-yu-like and midsummer-like periods (Figs. 12 and 13). For the mei-yu-like (pentads 32–39, from early June to mid-July) period in the idealized land-only simulation (Figs. 12a and 13a) there is a subtropical high to the east over the ocean, and a monsoonal flow that brings high moist static energy air to the southeastern portion of the continent and hence rainfall. North of this is the westerly regime, bringing low moist static energy air from the continental interior. As the season progresses to the midsummer-like period (pentads 40–43; from mid-July to early August), the high moist static energy region near the eastern coastline migrates northward and the rainfall migrates along with

it; this is accompanied by the northward expansion of the subtropical high, and with it the northern migration of the boundary of the westerlies (Figs. 12b and 13b).

This picture changes dramatically with the addition of a Tibetan-like plateau on top of the subtropical land. The mei-yu-like period (Figs. 12c and 13c) features a tilted rainband structure extending from just downstream of the plateau northeastwards out in the ocean. The rainfall itself is also more intense than in the idealized land-only simulation, because of the stronger tropical southerly flow as indicated by a larger zonal contrast between the 925-mb geopotential height just east of the plateau, with the subtropical high to the east (Fig. 12c). The introduction of the plateau brings about enhanced convection over the southern portion of the plateau (Fig. 13c), and the stronger southerly flow is consistent with it being forced by the resulting diabatic heating (Wu et al. 2007). This southerly flow is bounded to the north where it is met by a northerly flow from north of the plateau, bringing cold and dry air; the convergence in the lower troposphere marks the location of the rainband structure. When the midsummerlike stage is reached (Figs. 12d and 13d), the rainfall has shifted northward, and widens slightly. The subtropical high extends northward (as in the land-only case), allowing for an increased northward penetration of high moist static energy air over land to the east of the plateau. The northerly flow at the northern edge of the plateau, while still apparent, is much reduced compared to the mei-yu-like period; thus, there is less of a meridional convergence in the lower troposphere and therefore a somewhat wider rainband.

We further examine the direct effect of the plateau with an additional run where only the plateau is embedded in the base aquaplanet state. Results (Figs. 12e,f and 13e,f) show the presence of the subtropical high to the east of the plateau, despite there being no continentalsized land present; a similar result was found by Takahashi and Battisti (2007). However, unlike the idealized landonly simulation where the southerlies occur at the eastern edge of the subtropical land, in the idealized plateau-only simulation the strongest southerly flow occurs just off the eastern edge of the plateau; this flow resembles a lowlevel jet hugging its eastern boundary (Figs. 12e,f), reminiscent of the Great Plains low-level jet over North America (Higgins et al. 1997). Note that the convection over the southern edge of the plateau is vastly reduced as compared to the idealized land + plateau simulation, and thus does not explain the origins of the southerlies in the plateau-only simulation; rather, those southerlies are a direct consequence of the plateau itself. Thus, the low-level monsoon-like flow in the full land + plateau simulation arises from a combination of the land-ocean



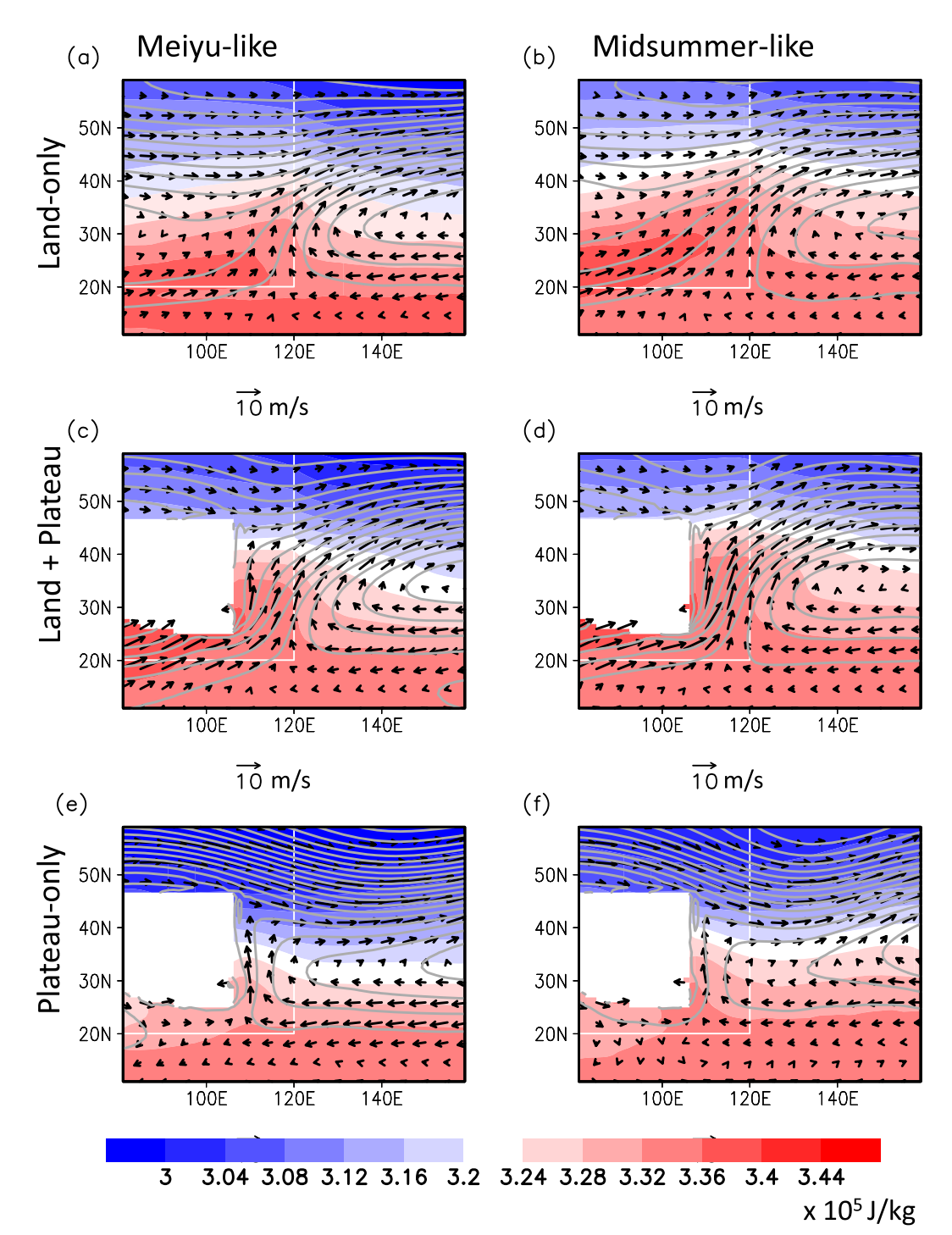


FIG. 12. Lower tropospheric (925 mb) fields of geopotential height (gray lines; contour interval is 15 m), moist static energy (shaded; $\times 10^5 \, \mathrm{J \, kg^{-1}}$), and winds (reference vector is $10 \, \mathrm{m \, s^{-1}}$). Idealized land-only simulation averaged over (a) pentads 32–39 and (b) pentads 40–43. (c),(d) As in (a) and (b), respectively, but for the idealized land + plateau simulation. (e),(f) As in (a) and (b), respectively, but for the idealized plateau-only simulation. The white line demarcates the land boundary; for (e) and (f) there is no land apart from where the plateau is imposed, so the lines are for reference only. The white box denotes the area covered by the plateau.

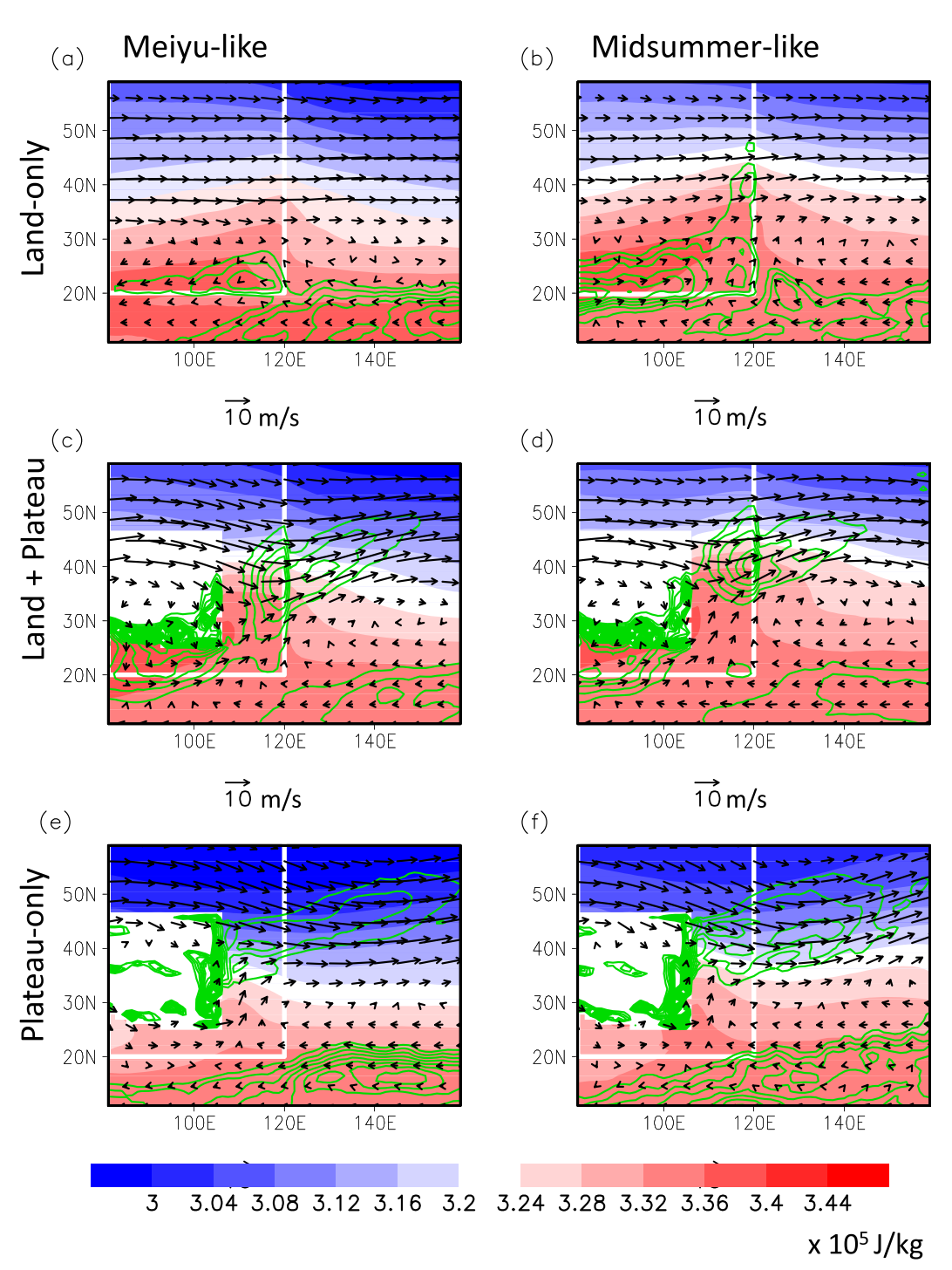


FIG. 13. As in Fig. 12, but for rainfall (green contours, see end of caption for contouring information); 925-mb moist static energy (shaded; $\times 10^5 \, J \, kg^{-1}$); and 500-mb winds (reference vector is $10 \, m \, s^{-1}$). Idealized land-only simulation averaged over (a) pentads 32–39 and (b) pentads 40–43. (c),(d) As in (a) and (b), respectively, but for the idealized land + plateau simulation. (e),(f) As in (a) and (b), respectively, but for the idealized plateau-only simulation. For rainfall, the contour interval is $0.5 \, mm \, day^{-1}$ for (a), (b), (e), and (f); for (c) and (d), it is $1 \, mm \, day^{-1}$. In all cases, only rainfall above $4 \, mm \, day^{-1}$ is shown.

contrast, convective heating at the southern edge of the plateau, and from direct influence by the plateau, with the first two responsible for the tropical southerly flow away from the eastern edge of the plateau (contrast Figs. 12a,b with Figs. 12e,f). Without the influence of the land-ocean contrast and convective heating at the southern edge of the plateau, moisture transport to the rainband will be reduced, and this is reflected in the relatively low rainfall within the rainband in the plateau-only simulation (Figs. 13e,f).

There are unrealistic aspects of the idealized simulations compared to observations, precluding a more definitive comparison to reality; in particular, the meridional migration of the rainfall in the idealized land + plateau simulation is muted compared to more realistic simulations. Regardless, the qualitative structure is apparent, and there is a mei-yu-like northward migration. There are clearly other factors to be considered, such as the influence of the Yunnan Plateau or the role of the South Asian monsoon. This exploration will be left to a future study.

7. Summary and discussion

The East Asian summer monsoon is distinct from other monsoons in the unique intraseasonal stages and abrupt transitions between them. This study examines the origins of the unique seasonality of the East Asian monsoon using an atmospheric general circulation model that simulates the seasonal transitions with fidelity. We start from the hypothesis posed by Molnar et al. (2010) that the intraseasonal stages result from the downstream effects of the westerlies impinging on the Tibetan Plateau, and how they change as the westerlies migrate north as the season evolves. The central role of the plateau is confirmed in a simulation that removes it as a boundary condition; this leads to convective rainfall over southeastern China with only one stage, as expected of a "conventional" monsoon. As the plateau is "grown," the intraseasonal stages emerge and the rainfall intensifies. The change to the character of rainfall is largely due to the emergence of large-scale rainfall resulting from the downstream stationary eddy circulation induced by the plateau.

We expand the original hypothesis proposed by Molnar et al. (2010) for how the plateau sets up the premei-yu through midsummer stages. As already detailed in Molnar et al. (2010), during the spring the westerlies straddle the plateau latitudinally, splitting the westerlies into a northern and southern branch. They reconverge downstream over East Asia, bringing cold dry air from the north to meet with warm moist air from the south, producing a humidity front (Fig. 9a) and rainband

structure. There is a mechanical lifting of the warmer and moister southerly flow, bringing about the persistent spring rains. During the pre-mei-yu, the westerlies begin to shift northward across the plateau. The extratropical northerlies are still present, but farther south a low-level southerly monsoonal flow emerges that brings moisture across the South China Sea toward southeastern China, bringing about the onset of convective rainfall there. The tropical monsoonal flow meets with the extratropical northerlies, intensifying the lower-tropospheric convergence, humidity front, and frontal rainband.

At mei-yu onset, the westerlies have shifted to the northern edge of the plateau such that the extratropical northerlies over northeastern China start to weaken; at the same time, the low-level monsoonal southerlies strengthen, driven by increased land-ocean contrast and South Asian monsoon heating. As a result, the locus of lower-tropospheric convergence, the humidity front, and the mei-yu rainband all migrate northward. At the onset of the midsummer stage, the westerlies have shifted sufficiently north to be clear of the influence of the plateau, and the extratropical northerlies over northeastern China disappear (Fig. 9d). As such, the monsoonal low-level winds, now unimpeded by the extratropical northerlies, penetrate to northeastern China (Fig. 8b); the distinct rainband disappears and rainfall becomes largely convective in nature. Toward the end of the midsummer stage, the westerlies again migrate over the Tibetan Plateau heading southward; the extratropical northerlies reform over northeastern China (Fig. 8a), leading to the termination of the midsummer stage.

The key to the unique East Asian rainfall seasonality is the interaction between two distinct circulations: the subtropical monsoon circulation that strengthens and extend northward as summer progresses, and the extratropical northerlies that weakens as summer progresses. The former circulation is typical of subtropical monsoons (and augmented by South Asian monsoon heating), but the latter is unique to East Asia resulting from the effect of the Tibetan Plateau. Thus, the basic ingredients needed to produce an East Asian-like rainfall seasonality appears to be (i) a subtropical landmass and neighboring ocean to the east, to produce the subtropical monsoon, and (ii) a plateau-like feature to the west of the eastern coastline of this continent, embedded within the westerlies such that the latter straddles the plateau in the winter, but migrate to its north during the early summer and eventually away from the plateau's influence in the peak of summer. In this sense, it is remarkable that the plateau appears to be fortuitously positioned to generate the intraseasonal stages seen today.

Our recent work (Kong and Chiang 2019) investigated the dynamics of how the northerlies are generated due to the presence of the westerlies impinging on the Tibetan Plateau. The edge of the plateau, at around 40°N, appears to be a threshold latitude for the westerlies; when the peak westerlies at the longitudes of the plateau shifts poleward of 40°N, the extratropical northerlies weaken, resulting in the termination of the mei-yu stage. The current study expands on this framework to encompass the entire seasonal evolution of the East Asian summer monsoon. Like Kong and Chiang (2019), we posit a fundamental role for the westerlies impinging on the plateau, and associated extratropical northerlies downstream, to determine the various intraseasonal stages. We are still unclear regarding the relative roles of mechanical forcing, thermal heating by the plateau, and land-ocean contrasts in driving the extratropical northerlies, and tropical southerlies; this will be a focus of future research.

While we have emphasized the role of the extratropical northerlies in this study, other studies focusing on the mei-yu rainband have emphasized different aspects of the large-scale circulation as key. In particular, Sampe and Xie (2010) emphasized the advection of warm air from the southern edge of the Tibetan Plateau by the westerlies as key to the existence and maintenance of the rainband. A reviewer suggested that the ageostrophic secondary circulation associated with the confluence of upper-level westerly flows is responsible for the uplift associated with the mei-yu rainband, given that the former is tied to an ageostrophic upper-level southerly flow with downward flow to the north and upward flow to the south. This explanation might explain rainfall in the spring stage when there is a split jet around the plateau and reconvergence downstream (see Fig. 4a), but is less relevant for the summer rainfall stages since the jet core shifts to the north side of the plateau (Figs. 4b-e). Others have focused on the role of the western North Pacific subtropical high and its northward expansion as key to the seasonal evolution (Ding 2004). We have not explored these alternative views here, but it would be worth doing so. In the end, the veracity of our hypothesis will depend on its ability to explain these other key features of the East Asian monsoon seasonality. However, our hypothesis is able to explain the zeroth-order features of the East Asian monsoon, including the complex seasonality that is unique among Earth's monsoon systems.

Acknowledgments. We acknowledge high-performance computing support for the CAM5 from the Cheyenne cluster (https://doi.org/10.5065/D6RX99HX) provided by NCAR's Computational and Information Systems

Laboratory, sponsored by the National Science Foundation. This work was supported by National Science Foundation Grant AGS-1405479, and Department of Energy Grant DE-SC0014078; DSB was supported by funds from the Tamaki Chair. We thank Huang-Hsiung Hsu, Peter Molnar, Inez Fung, and Jiabin Liu for useful discussions, and Walter Hannah for sharing his experience on his blog (http://hannahlab.org) regarding setting up the aquaplanet configuration of CESM. Topography boundary conditions and model output used in this paper are archived in Chiang et al. (2018).

REFERENCES

- Abe, M., A. Kitoh, and T. Yasunari, 2003: An evolution of the Asian summer monsoon associated with mountain uplift—Simulation with the MRI atmosphere–ocean coupled GCM. *J. Meteor. Soc. Japan*, **81**, 909–933, https://doi.org/10.2151/jmsj.81.909.
- Bolin, B., 1950: On the influence of the Earth's orography on the general character of the westerlies. *Tellus*, **2**, 184–195, https://doi.org/10.3402/tellusa.y2i3.8547.
- Boos, W. R., and Z. M. Kuang, 2010: Dominant control of the South Asian monsoon by orographic insulation versus plateau heating. *Nature*, 463, 218–222, https://doi.org/10.1038/nature08707.
- —, and —, 2013: Sensitivity of the South Asian monsoon to elevated and non-elevated heating. *Sci. Rep.*, **3**, 1192, https://doi.org/10.1038/srep01192.
- Chen, J., and S. Bordoni, 2014: Orographic effects of the Tibetan Plateau on the East Asian summer monsoon: An energetic perspective. *J. Climate*, **27**, 3052–3072, https://doi.org/10.1175/JCLI-D-13-00479.1.
- Chiang, J. C. H., and Coauthors, 2015: Role of seasonal transitions and westerly jets in East Asian paleoclimate. *Quat. Sci. Rev.*, **108**, 111–129, https://doi.org/10.1016/j.quascirev.2014.11.009.
- —, L. Swenson, and W. Kong, 2017: Role of seasonal transitions and the westerlies in the interannual variability of the East Asian summer monsoon precipitation. *Geophys. Res. Lett.*, 44, 3788–3795, https://doi.org/10.1002/2017GL072739.
- ——, W. Kong, C.-H. Wu, and D. S. Battisti, 2018: Data from: Origins of East Asian summer monsoon seasonality, v4 [dataset]. UC Berkeley, accessed 27 December 2019, https://doi.org/10.6078/ D19M21.
- —, J. Fischer, W. Kong, and M. J. Herman, 2019: Intensification of the pre-Meiyu rainband in the late 21st century. *Geophys. Res. Lett.*, 46, 7536–7545, https://doi.org/10.1029/2019GL083383.
- Day, J. A., I. Fung, and W. Liu, 2018: Changing character of rainfall in eastern China, 1951–2007. *Proc. Natl. Acad. Sci. USA*, 115, 2016–2021, https://doi.org/10.1073/pnas.1715386115.
- Ding, Y. H., 2004: Seasonal march of the East-Asian summer monsoon. East Asian Monsoon, C. P. Chang, Ed., World Scientific, 3–53.
- ——, and J. C. L. Chan, 2005: The East Asian summer monsoon: An overview. *Meteor. Atmos. Phys.*, **89**, 117–142, https://doi.org/10.1007/s00703-005-0125-z.
- Flohn, H., 1957: Large-scale aspects of the "summer monsoon" in South and East Asia. *J. Meteor. Soc. Japan*, **35A**, 180–186, https://doi.org/10.2151/jmsj1923.35A.0_180.
- ——, 1960: Recent investigations on the mechanism of the 'summer monsoon' of southern and eastern Asia. *Monsoons of the World*, S. Basu et al. Eds., India Meteorological Department, 75–88.

- ——, 1968: Contributions to a meteorology of the Tibetan highlands. Atmos. Sci. Paper 130, Dept. of Atmospheric Science, Colorado State University, 128 pp.
- He, H. Y., J. W. Mcginnis, Z. S. Song, and M. Yanai, 1987: Onset of the Asian summer monsoon in 1979 and the effect of the Tibetan Plateau. *Mon. Wea. Rev.*, 115, 1966–1995, https://doi.org/10.1175/ 1520-0493(1987)115<1966:OOTASM>2.0.CO;2.
- Higgins, R., Y. Yao, E. Yarosh, J. E. Janowiak, and K. Mo, 1997: Influence of the Great Plains low-level jet on summertime precipitation and moisture transport over the central United States. J. Climate, 10, 481–507, https://doi.org/10.1175/1520-0442(1997)010<0481:IOTGPL>2.0.CO;2.
- Hurrell, J. W., and Coauthors, 2013: The Community Earth System Model: A framework for collaborative research. *Bull. Amer. Meteor. Soc.*, 94, 1339–1360, https://doi.org/10.1175/BAMS-D-12-00121_1
- Kalnay, E., and Coauthors, 1996: The NCEP/NCAR 40-Year Reanalysis Project. Bull. Amer. Meteor. Soc., 77, 437–471, https://doi.org/10.1175/1520-0477(1996)077<0437:TNYRP> 2.0.CO:2.
- Kitoh, A., 2004: Effects of mountain uplift on East Asian summer climate investigated by a coupled atmosphere-ocean GCM. J. Climate, 17, 783–802, https://doi.org/10.1175/1520-0442 (2004)017<0783:EOMUOE>2.0.CO;2.
- Kong, W., and J. C. H. Chiang, 2019: Interaction of the westerlies with the Tibetan Plateau in determining the mei-yu termination. J. Climate, 33, 339–363, https://doi.org/10.1175/JCLI-D-19-0319 1
- —, L. M. Swenson, and J. C. Chiang, 2017: Seasonal transitions and the westerly jet in the Holocene East Asian summer monsoon. J. Climate, 30, 3343–3365, https://doi.org/10.1175/ JCLI-D-16-0087.1.
- Lenters, J., K. Cook, and T. Ringler, 1995: Comments on "On the influence of the Andes on the general circulation of the Southern Hemisphere." *J. Climate*, **8**, 2113–2115, https://doi.org/10.1175/1520-0442(1995)008<2113:COTIOT>2.0. CO:2.
- Li, C., and M. Yanai, 1996: The onset and interannual variability of the Asian summer monsoon in relation to land–sea thermal contrast. *J. Climate*, **9**, 358–375, https://doi.org/10.1175/1520-0442(1996)009<0358:TOAIVO>2.0.CO;2.
- Liang, X., Y. Liu, and G. Wu, 2005: The role of land-sea distribution in the formation of the Asian summer monsoon. Geophys. Res. Lett., 32, L03708, https://doi.org/10.1029/2004GL021587.
- Liu, Y. M., G. X. Wu, H. Liu, and P. Liu, 2001: Condensation heating of the Asian summer monsoon and the subtropical anticyclone in the Eastern Hemisphere. *Climate Dyn.*, 17, 327– 338, https://doi.org/10.1007/s003820000117.
- ——, B. Hoskins, and M. Blackburn, 2007: Impact of Tibetan orography and heating on the summer flow over Asia. *J. Meteor. Soc. Japan*, 85B, 1–19, https://doi.org/10.2151/jmsj.85B.1.
- Molnar, P., W. R. Boos, and D. S. Battisti, 2010: Orographic controls on climate and paleoclimate of Asia: Thermal and mechanical roles for the Tibetan Plateau. Annu. Rev. Earth Planet. Sci., 38, 77–102, https://doi.org/10.1146/annurev-earth-040809-152456.
- Park, H. S., J. C. H. Chiang, and S. Bordoni, 2012: The mechanical impact of the Tibetan Plateau on the seasonal evolution of the

- South Asian monsoon. *J. Climate*, **25**, 2394–2407, https://doi.org/10.1175/JCLI-D-11-00281.1.
- Rodwell, M. J., and B. J. Hoskins, 2001: Subtropical anticyclones and summer monsoons. *J. Climate*, **14**, 3192–3211, https://doi.org/10.1175/1520-0442(2001)014<3192:SAASM>2.0. CO:2.
- Sampe, T., and S.-P. Xie, 2010: Large-scale dynamics of the meiyu-baiu rainband: Environmental forcing by the westerly jet. *J. Climate*, 23, 113–134, https://doi.org/10.1175/ 2009JCLI3128.1.
- Schiemann, R., D. Lüthi, and C. Schär, 2009: Seasonality and interannual variability of the westerly jet in the Tibetan Plateau region. *J. Climate*, 22, 2940–2957, https://doi.org/10.1175/2008JCLI2625.1.
- Son, J. H., K. H. Seo, and B. Wang, 2019: Dynamical control of the Tibetan Plateau on the East Asian summer monsoon. *Geophys. Res. Lett.*, 46, 7672–7679, https://doi.org/10.1029/ 2019GL083104.
- Staff Members, 1957: On the general circulation over eastern Asia (I). *Tellus*, **9A**, 432–446, https://doi.org/10.1111/j.2153-3490.1957.tb01903.x. [The full authorship is given as "Staff Members of the Section of Synoptic and Dynamic Meteorology. Institute of Geophysics and Meteorology, Academia Sinica, Peking" and likewise for the next reference.]
- —, 1958: On the general circulation over eastern Asia (II). Tellus, 10A, 58–75, https://doi.org/10.1111/j.2153-3490.1958. tb01985.x.
- Takahashi, K., and D. S. Battisti, 2007: Processes controlling the mean tropical Pacific precipitation pattern. Part I: The Andes and the eastern Pacific ITCZ. J. Climate, 20, 3434–3451, https://doi.org/10.1175/JCLI4198.1.
- Wu, G., and Coauthors, 2007: The influence of mechanical and thermal forcing by the Tibetan Plateau on Asian climate. J. Hydrometeor., 8, 770–789, https://doi.org/10.1175/ JHM609.1.
- —, Y.-M. Liu, X.-Y. Zhu, W. Li, R. Ren, A. Duan, and X. Liang, 2009: Multi-scale forcing and the formation of subtropical desert and monsoon. *Ann. Geophys.*, 27, 3631–3644, https:// doi.org/10.5194/angeo-27-3631-2009.
- —, Y. Liu, B. Dong, X. Liang, A. Duan, Q. Bao, and J. Yu, 2012a: Revisiting Asian monsoon formation and change associated with Tibetan Plateau forcing: I. Formation. *Climate Dyn.*, **39**, 1169–1181, https://doi.org/10.1007/s00382-012-1334-z.
- ——, Y. M. Liu, B. He, Q. Bao, A. M. Duan, and F. F. Jin, 2012b: Thermal controls on the Asian summer monsoon. *Sci. Rep.*, **2**, 404, https://doi.org/10.1038/srep00404.
- Yanai, M., and G.-X. Wu, 2006: Effects of the Tibetan Plateau. *The Asian Monsoon*, B. Wang et al., Eds., Springer, 513–549.
- Yatagai, A., K. Kamiguchi, O. Arakawa, A. Hamada, N. Yasutomi, and A. Kitoh, 2012: APHRODITE constructing a long-term daily gridded precipitation dataset for Asia based on a dense network of rain gauges. *Bull. Amer. Meteor. Soc.*, 93, 1401– 1415, https://doi.org/10.1175/BAMS-D-11-00122.1.
- Yeh, T.-C., S. Tao, and M. Li, 1959: The abrupt change of circulation over the Northern Hemisphere during June and October. *The Atmosphere and the Sea in Motion*, B. Bolin, Ed., The Rockefeller Institute Press, 249–267.